MASTER THESIS

Master degree in Advanced Materials Science and Engineering

UPCYCLING OPAQUE PET WASTE BY REACTIVE EXTRUSION

REPORT

Author:	Eric Hacksell
Director:	Orlando Onofre Santana Perez
Co-Director:	Jonathan Cailloux
Call:	February, 2021

Abstract

This work was performed as a part of the project RevalPET UP, a project aiming to find new ways of recycling opaque polyethylene terephthalate waste (rPET-O) into a new primary material.

Recently, white opaque PET has been used as a material for milk bottles in France. The bottles contain up to 15% titanium dioxide (TiO_2) nanoparticles, protecting the milk from UV degradation and gas permeation into the bottle. However, the presence of this material disrupts the recycling flow as it removes the transparency should it be mixed with transparent PET as well as its mechanical properties being insufficient to become a new primary material on its own.

Reactive extrusion with a chain extender agent can be used to improve the properties of this material. In this work, the reactive extrusion of rPET-O with the multifunctional epoxydic oligomer Joncryl ADR 4400 was investigated at 0, 1 and 1.5wt%. The rotation speed of the screws for the twin-screw extruder were also varied between 40rpm and 80rpm.

It was found that the intrinsic viscosity increased the most for 1wt% addition of chain extender, while the rotation speed did not matter for this property. The melting temperature and crystallisation temperature was slightly decreased after reactive extrusion but did not change with Joncryl concentration nor with different screw rotation speeds. The complex viscosity and storage modulus were the highest for 1wt% Joncryl and a rotation speed of 40rpm, indicating that these conditions made the chain externder and the rPET-O react the most. The elongation at break increased the most with 1wt% addition of Joncryl, as the material gained the ability to strain harden after necking. The addition of 1.5wt% Joncryl chain extender made the material brittle.

Resumen

Este trabajo se realizó en el marco del proyecto RevalPET UP, cuyo objetivo es encontrar nuevas formas de reciclar los residuos de tereftalato de polietileno opaco (rPET-O) para convertirlos en uno nuevo material primario.

Recientemente, el PET blanco opaco se ha utilizado como material para las botellas de leche en Francia. Las botellas contienen hasta un 15% de nanopartículas de dióxido de titanio (TiO2), que protegen la leche de la degradación por los rayos UV y de la permeación de gases en la botella. Sin embargo, la presencia de este material perturba el flujo de reciclaje, ya que elimina la transparencia en caso de que se mezcle con el PET transparente, además de que sus propiedades mecánicas son insuficientes para convertirse en un nuevo material primario por sí solo.

La extrusión reactiva con un agente extensor de cadena puede utilizarse para mejorar las propiedades de este material. En este trabajo se investigó la extrusión reactiva de rPET-O con el oligómero epoxídico multifuncional Joncryl ADR 4400 al 0, 1 y 1,5wt%. También se varió la velocidad de rotación de los tornillos de la extrusora de doble tornillo entre 40rpm y 80rpm.

Se comprobó que la viscosidad intrínseca aumentaba al máximo con la adición de 1wt% de extensor de cadena, mientras que la velocidad de rotación no era importante para esta propiedad. La temperatura de fusión y la temperatura de cristalización disminuyeron ligeramente tras la extrusión reactiva, pero no cambiaron con la concentración de Joncryl ni con las diferentes velocidades de rotación del tornillo. La viscosidad compleja y el módulo de almacenamiento fueron los más elevados para el 1wt% de Joncryl y una velocidad de rotación de 40rpm, lo que indica que estas condiciones hicieron reaccionar más al extensor de cadena y al rPET-O. El alargamiento a la rotura fue el que más aumentó con la adición de 1wt% de Joncryl, ya que el material adquirió la capacidad de endurecerse por deformación tras el cuelgue. La adición de 1,5wt% de extensor de cadena Joncryl hizo que el material se volviera frágil.

Acknowledgements

First, I would like to thank my director, Dr. Orlando Onofre Santana Perez for giving me the opportunity to work on this project, and to discover a new field and learn more deeply about this. Thank you to my co-director, Dr. Jonathan Cailloux, for the training, the explanations of theoretical concepts, the guidance given and proof-reading of this report.

I would also like to thank Dr. Maria Lluïsa Maspoch Ruldua for allowing the equipment and machines of the Centre Catalá del Plàstic to be used in this project. Thank you, David Loaeza, for the support you have given during this project, the training and practical everyday tips about life in the laboratory. Y también para haber sido mi profe de español durante estos cinco meses, claro.

Thank you, Dr. Tobias Abt, for helping me with making my way around the machines in the laboratory and some useful practical tips. I hope the thermoplastic composites you told me about sees the market soon.

Not to be forgotten are my fellow master students, Laetitia Santarini and Hector Jeannot, with whom I work alongside I have spent most lunchtimes with and for being there to exchange both intellectual and unintellectual ideas with. Best of luck in the future for you both.

Thank you to my family and my girlfriend for having been supportive, especially during the last moments of this thesis. Vi ses snart! Yakında görüşeceğiz!

Table of contents

Preface

1.1. Origin of work

This work has been carried out as part of the project "Reevaluation of recycled opaque PET in innovative materials", **RevalPET'UP**, financed by FEDER funds through the POCTEFA programme, a transborder programme between Spain, France and Andorra. The different institutions working within the project RevalPET'UP are:

University of Zaragoza (UNIZAR), Spain
University of Pau and Pays de l'Adour (UPPA), France
University of the Basque Country (UPV), Spain
National Engineering School of Tarbes (ENIT), France
ePLASCOM research group, Polytechnic University of Catalonia (UPC), Spain

The work presented in this master's thesis was performed in CCP-UPC. All institutions play different roles in making sure the goal of the project is reached, as they all have different specialisations. The goal is to reduce the environmental impact of plastic products by upcycling opaque PET waste material into new, innovative materials. It falls in the common goal of the European union of using recycled or renewable raw materials and sustainable manufacturing technologies.

The main objective of this work is to analyze the morphology and mechanical and thermal properties of recycled, opaque polyethylene terephthalate (rPET-O) and then compare them with those of structurally modified rPET-O, compounded rPET-O with a multiepoxic agent through the use of reactive extrusion. In the goal of optimizing processing conditions, the concentration of the multiepoxic agent and the rotation speed of the screws during extrusion will be the two independent variables investigated.

To this end, these specific objectives are defined:

1. Preparation of materials at a pilot plant scale (maximum 5kg/h)
    a) Homogenisation of rPET-O flakes through the use of a single-screw extruder, producing rPET-O pellets.
    b) Reactive extrusion of the homogenized material using a multiepoxy agent.
    c) Compression moulding of the pellets using a hot platen press to produce thin plates of each material.

2. Chemical characterisation

    Determination of intrinsic viscosity of the acquired materials following the norm ISO 527:2. The objective is to estimate the viscosity average molecular weight.

3. Rheological characterisation

    Determination of the complex viscosity for low frequency oscillating shear forces through the use of rotational rheometry.

4. Thermal characterisation

    Determine the characteristic thermal transitions and degree of crystallinity of the materials through Differential Scanning Calorimetry (DSC).

5. Mechanical characterisation

    Analyse the effect of the addition of chain extender and its processing conditions on the mechanical parameters by performing uniaxial tensile tests at constant crosshead displacement speed.

This work is a continuation of the work produced by A. Lapuyade Cejudo [1], working with the same material and multiepoxydic chain extender but using a different method for the reactive processing.

1.2. Motivation

Plastic materials have become a great part of our everyday life, food packaging, building and construction, clothes, and many more. They have become so integrated in our lives that imagining a future without them seems almost unimaginable. The versatility, formability and low-cost of plastic materials are what drive their success, however the negatives are not negligeable, as most plastics in the market currently are produced from fossil fuels and much of the waste ends up in landfills, not able to degrade in a natural environment. Treating this waste has become a relevant talking point in society, with the focus being on the recycling and the reusing of plastic waste. The benefits of recycling include less raw material production, lower energy consumption and lowering the amount of waste. In their 2019 report [2], PlasticsEurope stated, for the countries in EU28+NO/CH, that 56% of the plastics produced is being collected for end-of-life treatment. Of this treated plastic waste, 32.5% is recycled into new primary

material, 42.6% is incinerated for energy recovery and 24.9% goes to landfill. Promisingly, the landfill percentage steadily decreases every year [2].

One of the most recycled plastics in the world is polyethylene terephthalate, PET, with the average collection rate of PET bottles in Europe being 59.8%, some countries like Norway even showing as high as 97% [3]. Germany, the country in Europe with the most recycled PET in terms of tonnes, has a 93.5% collection rate [4].

Almost all of this is later mechanically recycled into new bottles, food packaging or polyester fiber for clothing. For the average customer, PET is usually seen in its transparent form, which poses little problems during recycling. While reprocessing the PET, it is subjected to high temperatures and degradation, which causes the average molecular weight to decrease along with its mechanical properties. However, using a certain percentage of recycled PET still produces products good enough for consumer purposes. The content of recycled PET (rPET) in new bottles is around 11%, with a goal of having 25% by 2025 and 30% by 2030. [5]

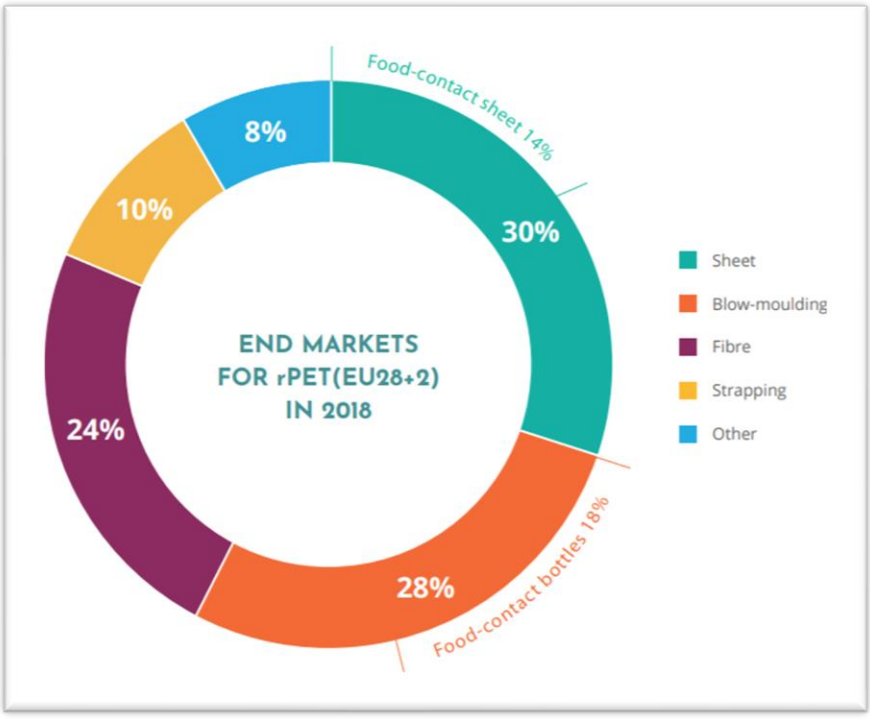

Figure 1. Distribution of recycled PET in Europe, 2018

Opaque recycled PET (rPET-O) has more recently entered the market as a way of protecting light-sensitive products such as UHT milk. [6] This is done mainly through the inclusion of titanium dioxide (TiO_2) in PET, a white powder pigment used to protect the PET from UV-degradation and to improve its processability. However, this has already posed problems in the recycling chain [6], as just a small quantity of opaque PET added to transparent PET will contaminate it and remove one of the desired properties of the material, its clarity and transparency. The properties of rPET-O are also not great, mainly due to TiO_2 microparticles. It was found that at a percentage of above 15% opaque PET, translating to 1.125% of TiO_2, the processability as well as the mechanical properties were too poor to be of any use [7]. The fibers produced from opaque PET break above this concentration of solid particles [8]. However, mixed with dark-coloured PET up to 15%, the fibers produced were considered strong enough. This means opaque PET has a more limited use, namely for clothing fibers and PET strappings. As recyclers must separate the two, the value and price of transparent rPET increases and makes it less appealing, which is counterproductive against the EU directive of wanting to increase and encourage recycling. In purely white PET bottles, an inclusion of up to 15% TiO_2 can be found in.

In France, more and more of this material is being used for bottles. The material that is traditionally used for white plastic bottles is PEHD. However, PET is lighter, more visually pleasing and above all, cheaper than PEHD. Given that it has a low recycling demand but at the same time is an increasingly present material it is destined to become a problem. Recyclers have suggested to stop using this material completely and instead cover the bottles with some sort of sleeve to fill the same function. This would facilitate the separation process and not disturb the recycling flow of today.

For now, there is waste produced that needs to be treated, and there are numerous ideas how to improve and use this material. For example, by adding the opaque PET waste to other polymers to produce blends, adding it in the form of fibres to other polymers or adding chain extenders to restore its quality. This project will be investigating the latter as an option for manufacturers to make this material more usable.

2. Theoretical aspects

2.1. Polyethylene terephthalate

Polyethylene terephthalate, PET, is a polymer that was first developed in 1941 by British Calico Printers and was designed to be used for synthetic fibres [9]. Later it was discovered that PET is a great material for

thin films as well for bottles. During the 1970s, the technique for blow moulding PET (bi-axially oriented) bottles was developed for commercial use and today this is the product that most people associate with PET. PET today is commonly found in clothes as polyester fibers, in bottles and food packaging and plastic films. For these applications, its advantages include transparency, barrier resistance to O_2 and CO_2, chemical inertness, resistance to wrinkling, resistance to fracture, lightweight and a high service temperature range [10]. Its market share of total polymer production is around 18% [2]. Even though the PET market is well established, research is being done to make the process cheaper and more environmentally friendly as well as improving the end-of-life treatment [11].

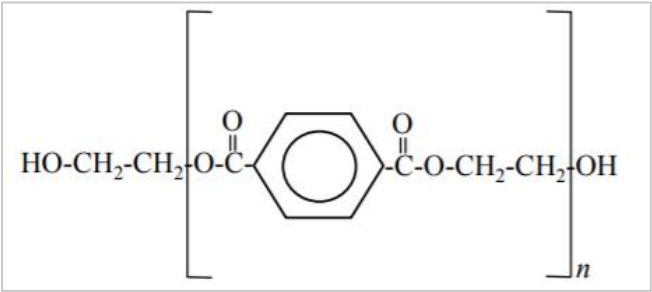

Figure 2. Chemical structure of PET.

There are different grades of PET, relating to their average molecular mass (given by measurements of its intrinsic viscosity) and their degree of crystallinity. Low molecular mass PET goes to the production of fibres while a higher molecular mass means the PET can be used for engineering purposes. For bottles production, a higher molecular mass as well as the PET being amorphous is required. Other properties remain the same no matter what grade PET is used, described in Table 1. [12]

Table 1. Characteristic properties of PET.

Density [g/cm^3]	**Glass transition temperature, T_g [°C]**	**Melting temperature, T_m [°C]**	**Young's Modulus, E [GPa]**	**Tensile Strength [MPa]**
1.38	70	250	2.8-3.1	50-150

2.1.1. Synthesis

PET can be derived in two different ways, the first one being from the direct esterification of ethylene glycol (EG) and terephthalic acid (TPA) [13]. It is being performed at a pressure of around 4 bar and a temperature of 240-260˚C, yielding the prepolymer Bis(hydroxyethyl) terephthalate (BHET) as well as

water [14]. According to Le Chatelier's principle, to produce more BHT it is necessary to evacuate the water molecules being produced. Hence why water is constantly being distilled out of the reactor.

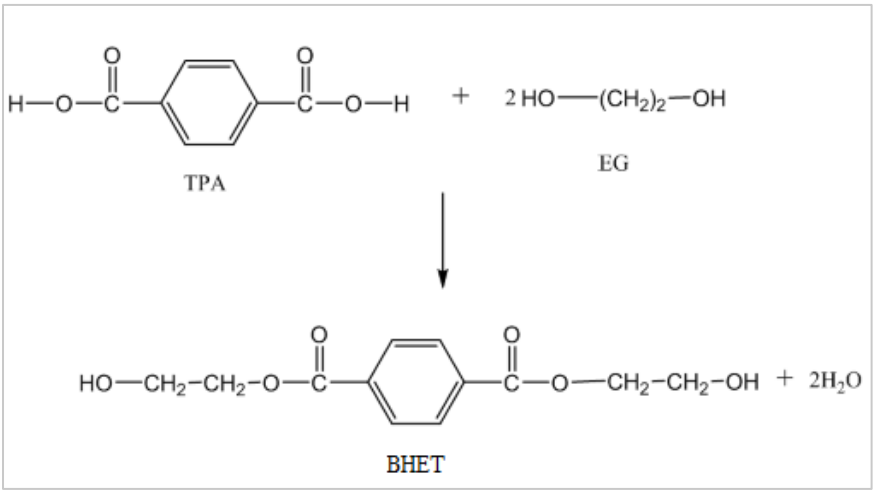

Figure 3. First step of PET synthesis; TPA esterification to produce BHET.

One unwanted by-product of this reaction is diethylene glycol. Decreasing the stochiometric relationship of EG to TPA and adding a small quantity of a strong base like sodium hydroxide both help in preventing this reaction from taking place. The BHET then undergoes a polycondensation reaction in the melt state where the PET chains can be formed alongside ethylene glycol. The figure below shows the reaction taking place.

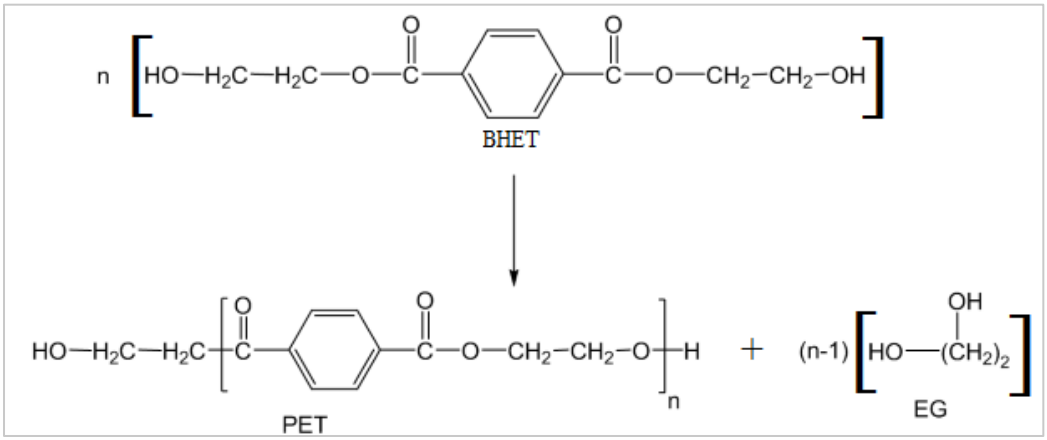

Figure 4. Final step in PET synthesis, polycondensation of BHET producing PET and EG.

For this polycondensation to be effective, evacuation of ethylene glycol from the system is necessary as it will shift the equilibrium to produce more PET. As EG has a higher volatility than BHET and PET, the process takes place in a high vacuum environment in order to diffuse it out of the mixture. A high surface-to-volume ratio of the reactor is also recommended to facilitate this diffusion.

The other way of producing BHET is using dimethyl terephthalate (DMT) instead of TPA. This process uses a slightly lower pressure and temperature to minimize the sublimination of DMT.

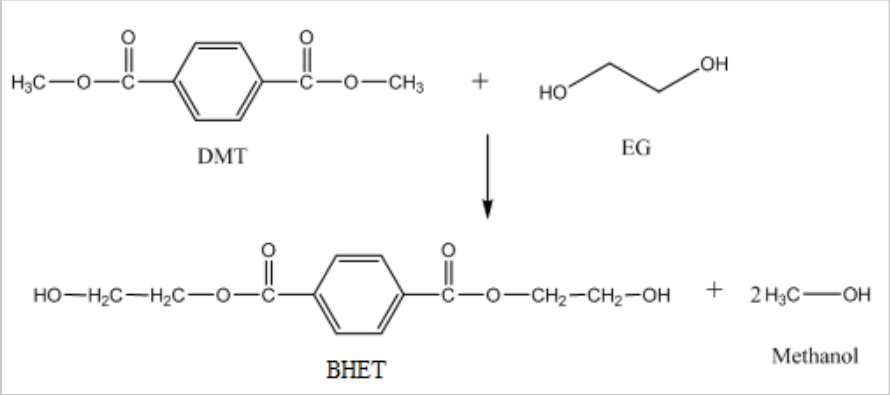

Figure 5. Chemical reactions to acquire the prepolymer BHET through the DMT method.

There are numerous advantages to using the TPA route over the DMT one. In their respective first steps, the EG/TPA ratio is significantly lower than the EG/DMT ratio. Therefore, in the shared second step, less amount of EG needs to be removed to achieve the same molecular weight. TPA also has a lower cost than DMT making it more economically beneficial.

2.1.2. Recycling

There are two ways that recyclers are using post-consumer waste PET, primary and secondary recycling. Primary recycling is when a certain percentage of rPET is being mixed with virgin PET to produce predominantly PET bottles. This is referred to as a closed loop and, when possible, is the preferred method [15]. Secondary recycling is when the material is downcycled to be used for fibres or strappings. This is the preferred way if the PET is not transparent as it could contaminate and diminish the desired transparency of PET bottles. Both ways of recycling use mostly mechanical recycling, consisting of first separating the

PET material from the waste stream, grinding the PET waste into flakes, washing and drying them and finally re-granulating through melting and reprocessing. The process creates the material rPET that can be used for manufacturing new PET products. During the final step, mechanical and thermal degradation of the PET can be caused by high temperatures and shear forces, causing a decrease in polymer chain length. This has the possibility to negatively influence material properties, such as crystallinity or mechanical strength. EU has created policies to encourage the recycling of PET and has decided that the percentage of rPET used in new PET bottles is to be a minimum of 25% by 2025, and 30% by 2030. [16]

Chemical recycling exists as well but is deemed too expensive to be viable at an industrial scale. This depolymerization directly leads to the formation of its constituent monomers. This is the recycling option more in line with circular economy and sustainable thinking, as it would nullify the need for fossil fuels and raw material in virgin PET production. The mechanisms through the recycling takes place are hydrolysis, methanolysis, glycolysis, ammonolysis, and aminolysis [17].

2.1.3. Degradation

Degradation in the environment has proven to be extremely slow, causing accumulation if it escapes the traditional waste stream or is littered [15]. However, as explained before, only a certain percentage of rPET can be mixed in with virgin PET to produce PET bottles. This is because degradation occurs, decreasing the average polymer chain length. The main mechanisms for degradation of PET are thermal degradation, oxidative degradation, and hydrolytic degradation [18].

The first step of thermal degradation is a scission of the ester bonds occurring randomly. This results in the formation of a vinyl ester as well as carboxyl end groups. This is then followed by a beta scission which forms acetaldehyde as well as increases the carboxyl end groups, further driving degradation.

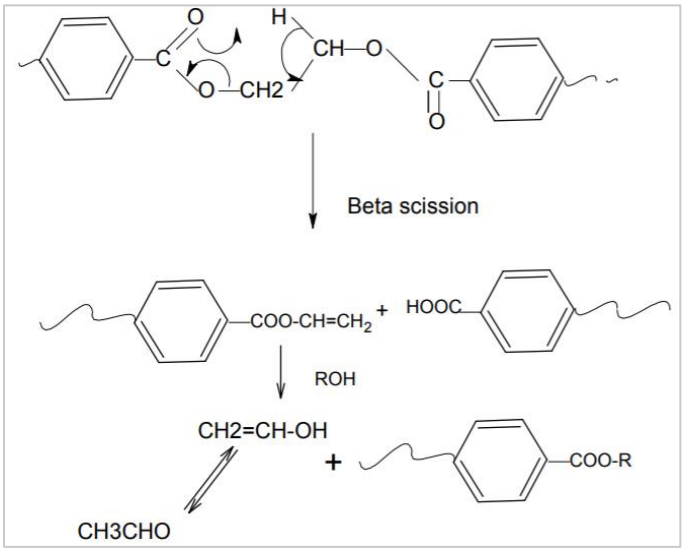

Figure 6. Schematic representation of thermal degradation.

For hydrolytic degradation, the factors affecting its rate is the presence of moisture as well as acid/alkaline impurities. The concentration of carboxyl end-groups increases the hydrolysis rate.

In 1997, Paci et al. showed that the most significant cause of degradation during processing is not the humidity of the PET before, but rather oxidation during processing [19]. This would mean that the most important factor to prevent degradation is using an inert atmosphere during processing. Often nitrogen gas is used for this purpose.

2.2. Blends

During recycling it is often the case that the plastic waste is hard to separate from one another. A classic case of this would be PET bottles which use bottle caps made from PP. Blending the two polymers together is the obvious solution, however this is not as easy as it sounds and can cause problems in the produced material. Most polymer blends are thermodynamically immiscible, causing phase separation. Mixing polar and non-polar polymers, as is the case for the PET/PP blend, will also lead to difficulties in dispersion of one of the phases, causing a heterogenous material [20]. They also have poor interfacial adhesion, leading to poor mechanical properties [21]. In immiscible blends, two different glass transition and melting temperatures would be seen during a DSC test. The main difficulty in achieving a good blend between two

polymers is their physical miscibility [22]. Titanium dioxide (TiO_2) is an additive commonly used in polymers but using them in PET/PP blends have shown to increase the interfacial tension between the droplet phase and the matrix. [23].

However, due to difficulties in separating different polymers during recycling, studies are being done to improve the quality of polymer blends. In PET bottles with PP caps, the caps could be removed to separate the two polymers. However, given the quantity of bottles in the recycling stream, this would be a laborious task. Mixing two polymers together can have benefits too, producing a new material with a combination of the important characteristics of each polymer. This line of thinking is akin to that of creating metal alloys, a common practice in the metal industry.

That is why studies have been done on making PET/PP blends feasible as a primary material. Studies are being done to optimise the proportion of each polymer in the blend as well as adding compatibilizers to decrease interfacial tension [22], [24], [25]. A method of improving the mechanical properties of these blends is to introduce grafted polymers. Grafters are block copolymers designed to reduce the interfacial tension between the two polymers, thereby achieving a more miscible blend. They have segments that are chemically similar or that have an affinity for the polymer [26]. PET/PP blends are using polypropylene grafted maleic anhydride (PP-g-MAH), maleic anhydride grafted styrene-ethylene/butylene-styrene (SEBS-g-MAH), polypropylene grafted acrylic acid (PP-AA), and ethylene vinyl acetate (EVA-g-MAH) based graft copolymers [22]. The grafted PP promotes a more finely dispersed phase, improves processability as well as modifies the crystallization behaviour of the PET. Akbari et. al showed that adding 10wt% of PP-g-MAH to a 70/30 PET/PP blend was the most effective for achieving the most finely dispersed PET phase [27]. Razak et. al did similar experiments and found that the tensile and flexural strength was at an optimum at 4wt% PP-g-MAH and the impact strength was improved significantly at 8wt% SEBS-g-MAH [22].

As this is an interesting field of study for the larger project RevalPET-UP in the goal of upcycling rPET-O, this has been the focus of other master's theses. In this project however, blends will not be explored as an option.

2.3. Polymer Chain Extenders and Reactive Processing

Since degradation occurs both naturally as well as during the processing of polymers, recycling the same material infinitely is not possible as the average molar mass will decrease over time. A way of compensating for the shortening of polymer chains is the use of chain extenders. The idea is to use a multifunctional compound with end-groups of the polymer you are interested in, re-joining the polymer chains, extending their length, and permitting branching [28]. Its addition to a polymer during processing increases the melt viscosity, improves the processability and improves the hydrolytic stability of the polymer in question. This is a method of upcycling post-consumer waste, increasing the number of times the material can be used. The method cannot however be used infinitely many times as degradation during processing decreases its mechanical properties.

To incorporate this material into a polymer, the materials together undergo something known as reactive processing. Simply explained, the base polymer and the reactive agent are mixed together and then inserted into either an internal mixer or a reactive extruder. There they experience blending through the help of rotors and high temperatures and react with each other. The residence time in the machine, the temperature, the rotor speed and the concentration of reactive agent all have an effect on the effectiveness of the reactive agent. One must also consider that the longer the polymer is in a high-temperature atmosphere, the more thermal degradation will occur. It is therefore a topic of research to optimise these conditions during reactive processing.

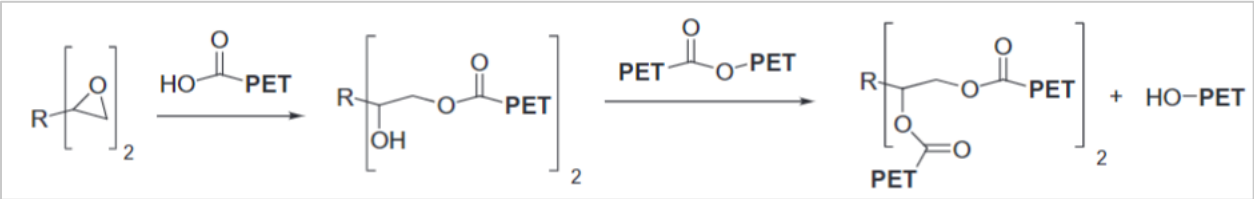

Figure 7. Chain extension and secondary branching reactions of PET with di-epoxides [29].

There are different kinds of chain extenders, namely bi-, tri- and multifunctional chain extenders. The bifunctional ones extend the polymer chains in a linear manner while the tri- and multifunctional ones promote crosslinking. For PET, extenders with reactive end groups are preferred, such as bisepoxy compounds, carboxylic dianhydride, and diisocyanates [30].

2.4. State of the art

The state-of-the-art section will provide previous scientific papers investigating reactive processing of PET with a structural modifier in the attempt to increase properties.

Table 2. State of the art of chain extension of PET

Author(s)	Main objective	Grade of PET	Reactive agent	Processing conditions	Results
D. Berg et al. (2018) [30]	Chain extension of PET with 1,3-phenylene-bis-oxazoline and N,N′-carbonylbiscaprolactam by reactive extrusion	Virgin PET, Maerkische Faser GmbH, Premnitz, Germany IV = 0.63 dL/g	1,3-phenylene-bis-oxazoline (1,3-PBO) N,N′-carbonylbiscaprolactam (CBC) 0.1, 0.2, 0.3, 0.5, 1.0, and 2.0wt%.	Micro 15 cc Twin Screw-Extruder T: 290°C rpm: 100 rpm	- Crystallinity and the lamellar thickness distribution of PET decrease with chain extenders. - Small concentrations did not effect thermal nor rheological properties. - All concentrations increased IV.
P. Raffa et al. (2012) [29]	Chain extension and branching of PET with bi- and multifunctional epoxy or isocyanate additives.	Postconsumer, coloured PET, SERIPLAST s.r.l., Firenze, Italy IV = 0.75 dL/g	**Bifunctional:** 1,6-diisocyanatohexane (NCO), Aldrich 0.5, 0,9, 1.3, 1.5 and 1.7wt% 1,4-butanediol diglycidyl ether, EPOX, Aldrich 0.6, 1.1, 1.56 and 2.04wt% **Multifunctional:** poly(phenyl isocyanate-co-formaldehyde) (P-NCO), Aldrich (multifuncional) 0.25, 0.5, 0.75 and 1wt.% Styrene-acrylatecopolymer bearing epoxide groups (P-EPOX)	Internal mixer: Brabender T: 270°C Rotor speed: 50 rpm Time of mix: 10 min.	- Bifunctional caused increase in Young's modulus, decrease in strain at break. Multifunctional opposite effect. - NCO showed higher reactivity than EPOX - Melt viscosity was increased while mechanical properties remained the same.
I S Duarte et al. (2016) [31]	Chain extension of virgin and recycled PET Effect of	Virgin PET, Cleartuf® Turbo™, Gruppo Mossi e	Joncryl, POLYAD PR-002, BASF Brazil 0.5, 1 and 1.5wt%	Internal mixer: Haake Rheomix 3000	- Low rotor speed is more suitable to avoid degradation.

	processing conditions and reprocessing	Ghisolfi, Brazil. IV = 0.88 dL/g Postconsumer PET Granplast, Recife PE, Brazil. IV = 0.72 dL/g		T: 260°C Time of mix: 20min Rotor speed: 30rpm, 60rpm, 120rpm	- 1.5wt% Joncryl increased molar mass, 1.0% - More Joncryl was needed for recycled PET than virgin PET. - Reprocessing PET with Joncryl led to less degradation than with pure PET.
K. Bocz et al. (2016) [32]	Low-Density Microcellular Foams from Recycled PET Modified by Solid State Polymerization and Chain Extension	Postconsumer PET, Jász-Plasztik Kft. Hungary IV = 0.71 dL/g Nucleating agent: HTPultra5 L type talc (T), IMI FABI SpA, Postalesio, Italy. Median diameter = 0.65µm	Joncryl ADR4368C, BASF SE, Ludwigshafen, Germany 6800 g/mol Epoxy eq. weight: 285 g/mol 0, 0.25, 0.5, 0.75, 1.0wt%	Labtech Scientific LTE 26-48 twin screw extruder Temp: 240–255 °C, Rotation speed: 100 rpm	- IV increased linearly and MFI decreased with an increase of Joncryl. - Void factor higher in reactive extrusion than solid state polymerization.
F N Cavalcanti et al. (2007) [33]	Chain extension and degradation during reactive processing of PET in the presence of TPP	Virgin PET, Rhopet S80, RhodiaSter S.A., Brazil Grade: Bottles for carbonated drinks Postconsumer PET (Repet, Brazil)	Triphenyl phosphite (TPP), Sigma Aldrich 1, 2 and 3wt%	Internal mixer: Haake-Buchler System 90 Torque Rheometer 260°C, 280°C, 300°C Time of mix: 30min Rotor speed: 60rpm	- 260°C, 1wt% TPP were the optimal processing conditions. - rPET less able to react with TPP than virgin PET
Y. Zhang et al. (2009) [34]	Influence of chain extension on the compatibilization and properties of rPET/LLDPE blends	Postconsumer PET, Zijiang Bottle Ltd., Shanghai, China IV = 0.71 dL/g. LLDPE, Panjin Polyethylene industry Co. Ltd. T_m = 126°C MI = 2.72 g/10 min (265 °C, 2.16 kg)	Polymeric methylene diphenyl diisocyanate (PMDI), Bayer Material Science AG With 30–32% isocyanate group 0, 0.5, 0.7, 0.9, 1.1wt% SEBS-g-MA, Kraton F1901X, Shell Chemical Company. 1.84 w% maleic anhydride	Co-rotating twin-screw extruder (L/D=48, D=35 mm) Zone 1 to 4 temperatures: 100°C, 150°C, 200°C and 240°C. Die temperature was 250°C	- Increase in PMDI content led to a decrease in crystallinity and an increase in T_g. - With 1.1wt% PMDI the impact strength increased greatly while tensile strength decreased slightly. - PET with PMDI in r-PET/LLDPE/ SEBS-g-MA blends decreased the compatibilization effect of SEBS-g-MA
A. Lapuyade	Characterisation of Opaque Recycled PET by means of Chain	Postconsumer transparent PET, unknown origin	Joncryl® ADR 4400, BASF SE,	Internal mixer:	- Opaque PET reacted more readily than

Cejudo (2020) [1]	Extender at Laboratory Scale, M.S. Thesis (in Spanish)	IV = 0.74 dL/g Postconsumer opaque, coloured PET, FLOREAL, Suez, Bayonne, France. IV = 0.64 dL/g	Ludwigshafen, Germany 0, 0.5, 1, 1.5wt%	Brabender Plastic-Corder W50EHT 260°C Time of mix: 35min Rotor speed: 50rpm	transparent PET with the reactive agent. - 1wt% Joncryl addition demonstrated the best mechanical properties. - 1wt% and 1.5wt% Joncryl in rPET-O did not dissolve in IV testing, suggesting crosslinking.

3. Materials used

This section will briefly describe the materials used for this project.

3.1. Recycled opaque PET flakes

The main material used in this master's thesis is recycled opaque PET flakes, commercial name FLOREAL, sent from the recycling company Suez in Bayonne, France. As can be seen in Figure 8, flakes with many different colours were included, both opaque and transparent ones. This is simply because in the recycling flow of today, the PET is first sorted and separated from other plastics and is then divided into a flow with transparent and un-coloured PET and another with coloured PET. Flakes of all colours are therefore mixed together.

Figure 8. Multi-coloured recycled PET flakes, commercial name FLOREAL, as they arrived.

As can be seen in Figure 8 there are many different colours in the base material, each presumably coming from a different product and source. In order to describe the composition of the recycled PET flakes, a simplification was made by classifying the different colours into various categories. The different categories were transparent un-coloured, transparent coloured, opaque coloured and opaque white flakes. It should be noted that some of the grey flakes, at times, contained a white part as well. However, they were still classified as opaque coloured flakes. In some cases, there was even pieces of paper and cotton that could be found. The sorting was not optimal either as some grey PET flakes had an inseparable white layer attached to them, making classification difficult (see Figure 9)

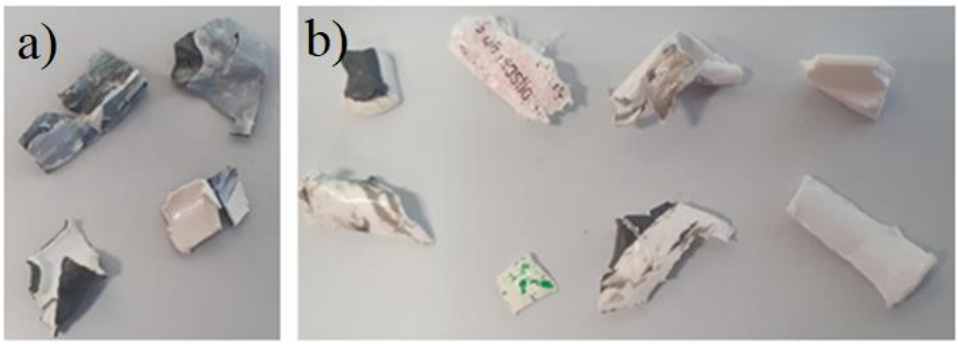

Figure 9. Artefacts from the recycled PET flakes in the base material. a) opaque coloured flakes. b) opaque white flakes.

To estimate the composition of the base material, 50 grams was taken at random and then sorted into each of the categories mentioned above and visualised in Figure 10, followed by each of them being weighed. The mass distribution of each category is found in Table 3.

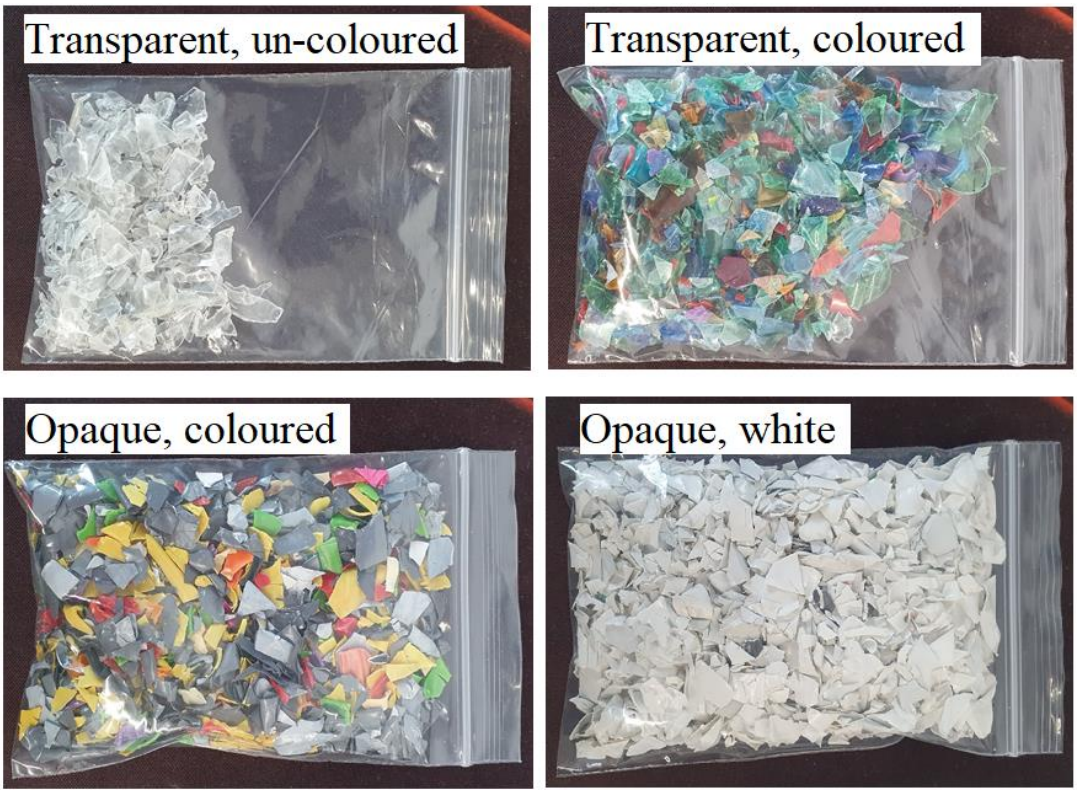

Figure 10. Categories of flakes from a 50g sample of the base material.

Table 3. Mass distribution of 50g of the base material.

	T, un-coloured	T, coloured	O, coloured	O, white
Mass (g)	4.652g	14.808g	13.065g	17.373g
wt% of total mass	9.32wt%	29.68wt%	26.18wt%	34.82wt%

Material of this same composition was used in the previous work [1] and through the method of calcination it was found that it contained 2.04wt% of inorganic particles.

3.2. Multifunctional epoxydic reactive agent

As stated earlier, the goal of of this project is to structurally modify rPET-O by increasing the average chain length. The reactive agent used for this purpose is Joncryl® ADR 4400, BASF Corporation, Ludwigshafen, Germany. Its chemical structure can be seen in the figure below.

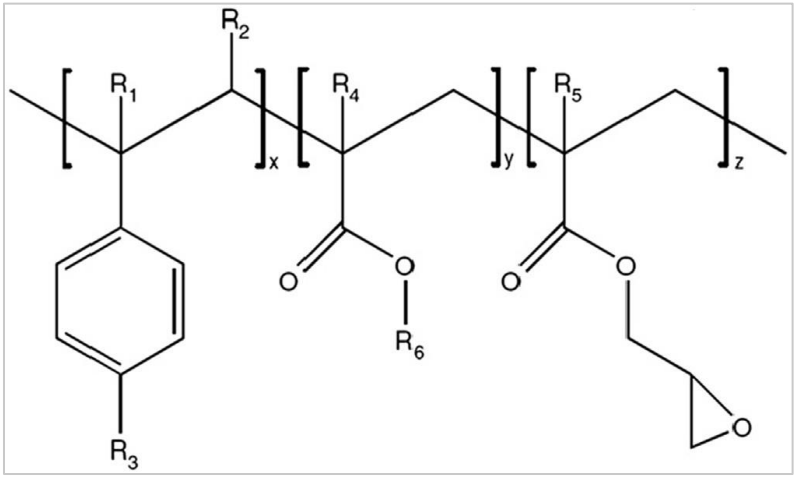

Figure 11. Molecular structure of Joncryl. x, y and z typically have values of between 4 and 10.

In the technical data sheet [35] for this multifunctional epoxydic oligomer is stated that it is primarily used for polyesters and can even be used for food contact applications. Table 4 describes the typical values displayed by this product, as described in the data sheet.

Table 4. Typical values for Joncryl® ADR 4400

Appearance	Specific gravity (25°C)	M_w	T_g	Epoxy equivalent weight (g/mol)	Number of epoxy groups per chain
Solid flakes	1.08	7 100	65°C	485	14-15

4. Processing methods

In this chapter the process of how each sample was obtained from the base material is explained. Both the production of pellets and the plates used for testing are detailed. The second part describes the characterisation methods used to analyse and compare the various thermal, mechanical, and chemical characteristics of each sample.

4.1. Homogenisation

To homogenize the material, first the multicoloured recycled PET flakes had to be dried in order to remove the residual moisture and minimise degradation during processing. In general it is desired that the moisture level of PET is below 50ppm before processing [36]. The material was therefore inserted into a dehumidifier at 120°C for 4 hours. The flakes were then inserted into a single screw extruder to be turned into pellets. The extruder is of model E-30/25, IQAP-LAP, Catalonia, Spain, with a screw diameter of 30mm and an L/D ratio of 25. The extruder had four heating zones along the profile of the screw, with their temperatures being set to 175/195/225/245ºC. To further minimise thermooxidative degradation, the extrusion was performed in a controlled atmosphere of N_2. The extruder was left to run for five minutes to get any impurities out of the machine, this step was to ensure that the extruded material was only rPET-O. Still in the molten state, the material from out the die was then quenched in two room temperature water baths, dried and then cut into pellets. The quenching permits the homogenised rPET-O to solidify faster and therefore be cut directly after drying, at the cost of freezing the microstructure in place and having amorphous rPET-O pellets.

Figure 12. Extrusion setup for homogenising recycled PET flakes.

Because of this, it was then recrystallised in an oven, 120˚C for four hours. This was done to increase the crystallinity up to 20-30%. After this step, the pellets for the reference material, rPET-O, had been fully prepared. These were also the pellets that were used for the preparation of the other materials, described in the next chapter. In total, 36kg was extruded, 24 of which was for partner universities.

Figure 13. Visual appearance of pellets after extrusion

4.2. Pilot plant reactive extrusion

The reactive extrusion process was conducted using a corotating twin screw extruder, model KNETER 25X36D, Collin, Maitenbeth, Germany. The extruder had seven heating zones, a L/D ratio of 36 and a screw diameter of 25mm. The temperature profile of these zones was set to 175/215/230/235/240/245/245°C. The extrusion is performed in vacuum to avoid further degradation as well as possible. Like in the extruder before, nitrogen gas was introduced to keep an inert atmosphere.

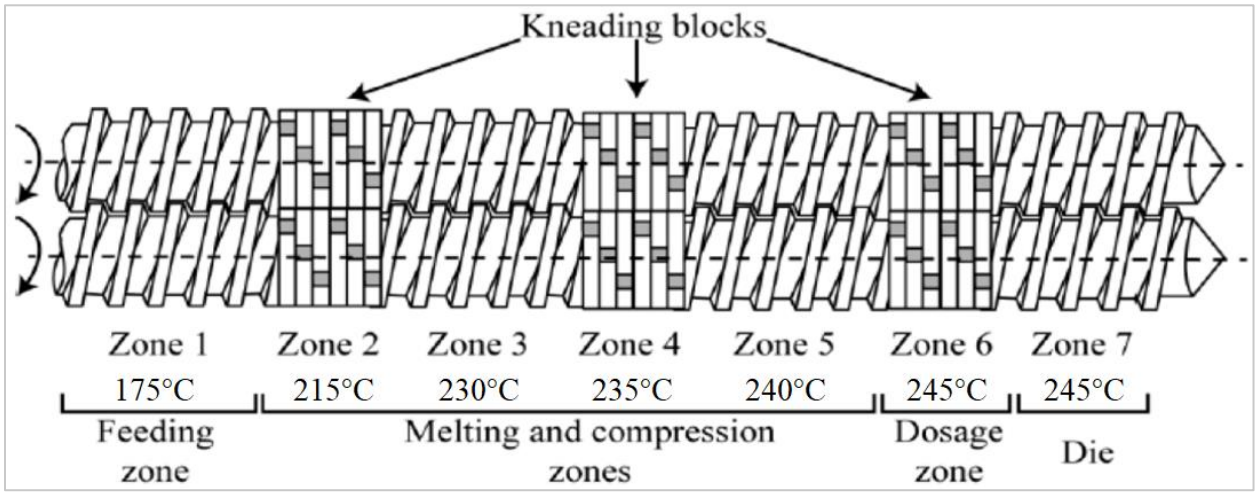

Figure 14. Schematic representation of the profile of the double screws used in the twin-screw extruder.

To avoid a heterogenous material in terms of varying Joncryl concentrations (Joncryl is the form of flakes while the rPET-O is in the form of pellets), pre-mixed batches of 100 grams were introduced one by one into the corotating twin screw extruder. The rotation speed of the screws was set to the predetermined conditions. After extrusion, the material was water cooled, dried and cut into pellets, after which the acquired material was once again recrystallised at 120˚C for four hours.

The objective is to evaluate the effect of the speed of the rotating screws as well as the degree of modification of rPET-O. For this purpose, two different speeds and two different Joncryl concentrations were used. The processed materials are described in Table 5.

Table 5. Description of the processing methods for each prepared material.

Material name	Concentration of Joncryl [wt%]	Rotation speed of the screws [rpm]

rPET-O+1J40	1	40
rPET-O+1J80	1	80
rPET-O+1.5J40	1.5	40

Each material was produced in large enough quantities to be able to conduct the experiments needed for this thesis. However, following results of the previous work [1], it was decided that rPET-O+1J40 was to be the focus during production. 18kg of this material was prepared, 12 of which was sent to partner universities.

4.3. Compression moulding

To be able to perform tensile testing and rotational rheology, thin plates measuring 15cm x 15cm were prepared from the materials described in Table 5. These were produced through compression moulding the pellets prepared earlier. According to the compression mould and theoretical density of the polymeric materials, 13.5 grams was used for each plaque and operating at a temperature of 270˚C produced the best results. Assuming that no material surpassed the edges, the average thickness of the plates was 0.44 mm.

The compression moulding machine used in this work was of model PL-15, IQAP-LAP, Maitenbeth, Germany, as seen in Figure 15.

Figure 15. Compression moulding machine, model PL-15, IQAP-LAP, used in this work.

The pellets were dried in a vacuum oven at 80°C for four hours to minimise the hydrolytic degradation caused by the heat and pressure from the compression moulding. Thermooxidative and thermal degradation is a potential problem since the compression is not done in an inert atmosphere. It is therefore desired to minimise the time spent for the entire compression process, while ensuring that the quality of the plates is sufficient.

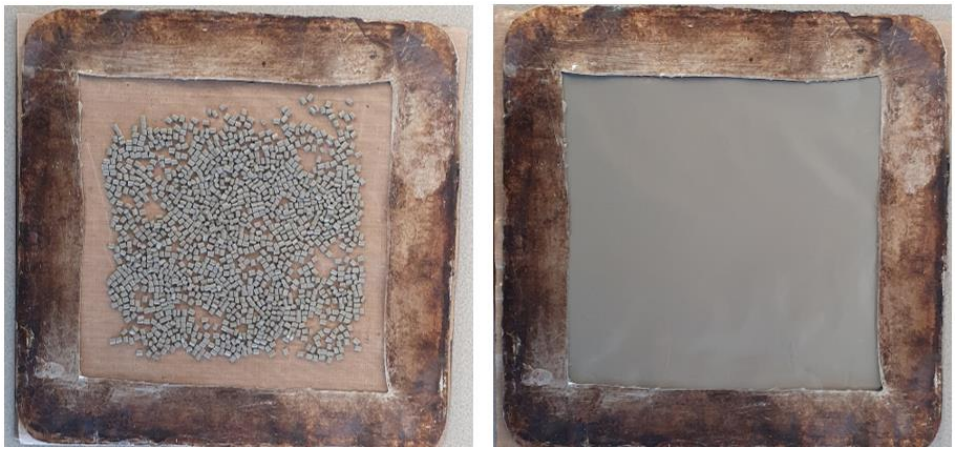

Figure 16. Steps of compression moulding. Before and after compression process.

The conditions for the compression moulding are described in Table 6. In total, the plates spent 4 minutes in the compression process, surely causing some degradation in the process. The pellets then followed a compression protocol as described in Table 7. The first compression at 0 bar was done to ensure the complete melt of the pellets before applying pressure. The melt could later be compressed at 20 and then 40 bar to fill out the mould homogenously. Between each compression step there was decompression to avoid the trapping of air bubbles. To avoid crystallising, fast cooling is needed to freeze the microstructure in place. For this purpose, the plates were quenched in ice water.

Table 6. Conditions of compression moulding.

Size of the plates	Material used [g]	Temperature [°C]	Total compression time [min]	Ice water quenching time [min]
15cm x 15cm	13.5g	270°C	4 min	1 min

Table 7. Compression protocol for production of plates.

Pressure [bar]	Time [min]
0	1 min
20	1 min
40	2 min

5. Experimental methods

In order to analyse the chemical, thermal and mechanical properties of the processed materials, various characterisation methods were used, these will be explained in this sub-chapter.

5.1. Intrinsic Viscosity (IV)

The intrinsic viscosity is defined by the ability of a polymer to increase the viscosity of a solvent. It is used to determine the average molecular mass and the topological structure of a polymer. The testing done for PET in this thesis follows the ASTM D4603-03 standard.

Once the polymer is dissolved into the solvent, the intrinsic viscosity is increased the greater the hydrodynamic volume of one polymer chain. The hydrodynamic volume describes the volume of a polymer coil in solution, depending on polymer chain length and the solvent used. However, it can also depend on the structure of the polymer, as heavily crosslinked polymer chains take up less space. [37]

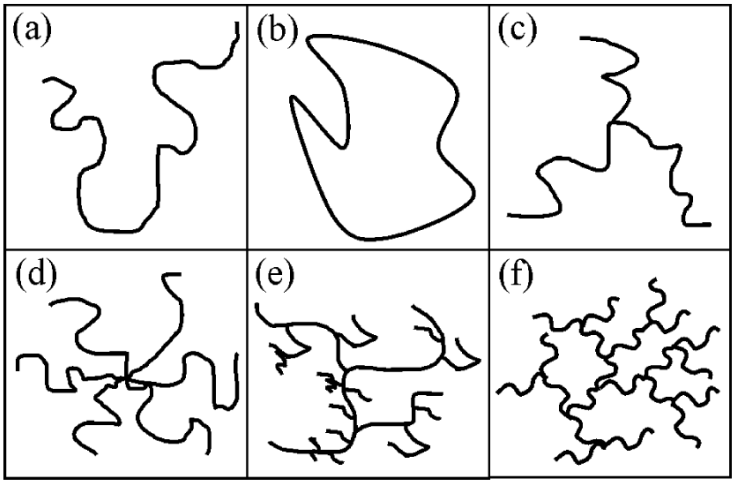

Figure 17. Schematic of molecular structures of a polymer: a) linear, b) ring, c) three-arm star, d) six-arm star, e) random hyperbranched, and f) dendrimers. [37]

As the reactive agent being used for reactive extrusion is a multifunctional chain extender, it is expected to crosslink the PET, more likely forming chains similar to the bottom row in Figure 17.

From the testing, three values are being directly measured. These are: concentration of dissolved polymer in solution (c) [g/dL], time taken for the solution to pass between two points in a capillary viscometer (t) [s], as well as the time taken for the pure solvent to pass between the same two points in a capillary viscometer (t_0) [s]. From these three measured values, various calculations are done. The equations [38] showing how to find the relative viscosity (η_{rel}), the inherent viscosity (η_{inh}), the reduced viscosity (η_{red}) and finally the intrinsic viscosity (η) are shown in equations 1-4:

$$\eta_{rel} = t/t_0 \quad \text{Eq. 1}$$

$$\eta_{inh} = \ln(\eta_{rel})/c \quad \text{Eq. 2}$$

$$\eta_{red} = (\eta_{rel} - 1)/c \quad \text{Eq. 3}$$

$$[\eta] = \frac{\eta_{red} + 3\eta_{inh}}{4} \quad \text{Eq. 4}$$

According to the ASTM D4603 standard, the concentration of dissolved PET, c, is 0.5 g/dL.

There are then equations describing the link between the intrinsic viscosity and the viscosity average molar mass, called Mark-Houwinks's equations. The general form of the equation is $[\eta] = KM^a$, with *K* and *a* being material and solvent based constants [39]. For PET dissolved in 60/40 phenol/1,1,2,2-tetrachloroethane (30˚C) the constants produce equations 5 and 6:

$$[\eta] = 3.72 \times 10^{-4}(\overline{M_n})^{0.73} \quad \text{Eq. 5}$$

$$[\eta] = 4.68 \times 10^{-4}\,(\overline{M_w})^{0.68} \quad \text{Eq. 6}$$

Rearranging these equations in order to determine the average molecular weight, $\overline{M_n}$, and the average molecular weight distribution, $\overline{M_w}$, consequentially produce the equations 7 and 8:

$$[\overline{M_n}] = (2688 \times \eta)^{1.37} \quad \text{Eq. 7}$$

$$[\overline{M_w}] = (2137 \times \eta)^{1.47} \quad \text{Eq. 8}$$

The samples were dried in a vacuum oven at 80°C overnight. After drying the examined PET sample was dissolved in the solvent 60/40 phenol/1,1,2,2-tetrachloroethane with a determined concentration of 0.5 g/dL. This was done at 110°C with continuous magnetic stirring for 15 minutes. If the polymer has solid particles, as was the case for rPET-O, it must undergo filtration. The remaining solution was then placed into an Ubbelohde glass capillary viscometer of type 1B, which was submerged into a water bath at 30˚C. This temperature was maintained constant throughout the experiment.

5.2. Rheometry

This experiment examines the molten-state behaviour and the viscoelasticity of a material and its response to shear forces. The sample is submitted to sinusoidal shear forces of varying frequencies while measuring the phase difference between applied force and responded deformation. From this, the complex viscosity (η*), the storage modulus (G´) and the loss modulus (G´´) can be calculated. The testing was performed on an AR-G2, TA Instruments, Philadelpia, United States.

Figure 18. AR G2 rheometer on which rheological tests were performed.

The upper plate is lowered to the lower plate with a known gap, followed by the upper plate oscillating with a low amplitude. The angular displacement of the sample is tracked at the same time. The relationship between stress and strain can then be plotted in order to get a phase difference, δ. In a purely elastic material, there would be no delay in response time, δ=0°, as the maximum stress would occur when there is maximum deformation. For a viscous material it would be 90° out of phase as the maximum stress would occur when the flow rate is the greatest. A viscoelastic material has an phase difference of 0°<δ<90°. This is visually represented in Figure 19. [40]

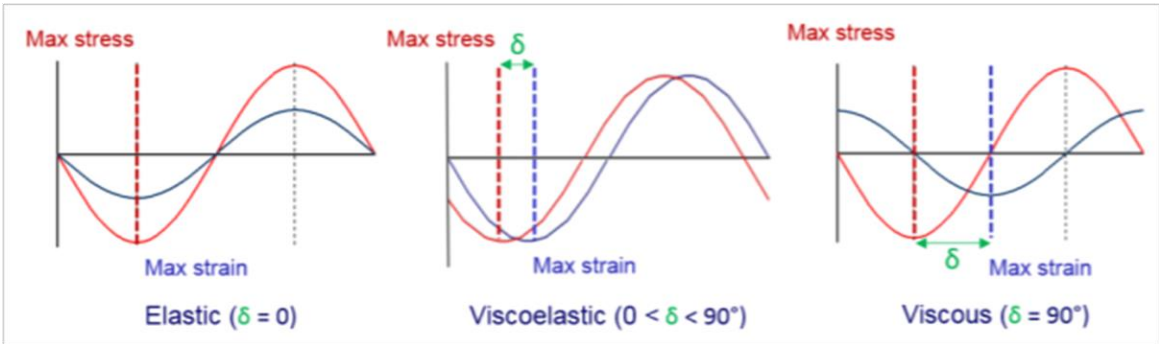

Figure 19. Relationship between applied stress vs. response in an elastic, a viscoelastic and a viscous material. [40]

To find the wanted characteristics, first the complex modulus (G*) is calculated.

$$G^* = G' + iG'' = \frac{\sigma_{max}}{\gamma_{max}} \quad \text{Eq. 9}$$

The elastic contribution to G* represents the storage of energy and is therefore named the storage modulus (G´), while the viscous contribution represents energy loss and therefore is named the loss modulus (G´´). They are both calculated in similar ways, as they both use the phase angle and the value of the complex modulus.

$$G' = G^* \times \cos(\delta) \quad \text{Eq. 10}$$

$$G'' = G^* \times \sin(\delta) \quad \text{Eq. 11}$$

The complex viscosity (η*) can then be found through a combination of the two moduli as well as taking into consideration the angular frequency (ω).

$$\eta^* = \frac{\sqrt{(G')^2+(G'')^2}}{\omega} \quad \text{Eq. 12}$$

Thanks to the empirically found Cox-Merz' rule [41], there is a correspondence in the graphs plotting the steady state shear viscosity (η) vs. the shear rate ($\dot{\gamma}$) and the plot for η* vs. ω.

$$\eta^*(\omega) = \eta(\dot{\gamma}) \quad \text{Eq. 13}$$

Circular samples of 25mm in diameter were cut out from the plates of each material. They were then put into a vacuum oven at 80°C overnight to dry. The sample was placed on the platform of the machine, enclosed in a nitrogen gas atmosphere chamber and heated to the testing temperature of 260°C. The parallel upper plate was ten lowered to 0.4mm to ensure contact during shear forces. The testing was then performed with a constant torque of 60 μN·m and a frequency ranging from 100 to 0.1 Hz, descending, with five data points per decade being collected.

5.3. Differential Scanning Calorimetry (DSC)

The Differential Scanning Calorimetry (DSC) test is designed to study the thermal behaviour of materials. It is used to detect and measure a material's various characteristic temperatures such as melting temperature and, for polymers in particular, the glass transition temperature. Every material has slightly different characteristic temperatures, as such the DSC test can also be used to identify the material.

The principle behind the test is that polymers, and other materials, have exothermic or endothermic events taking place at certain characteristic temperatures. For example, the crystallisation process of a polymer is exothermic because of the formation of bonds releasing energy. During DSC testing, a heat flow is supplied to the sample material as well as a reference material, while keeping the temperature of both materials equal. The different amount of heat supplied is then measured and plotted against temperature. In the resulting plot, characteristic temperatures of the sample material can be seen. The machine used in this work to perform DSC testing is DSC Q2000, TA Instruments, Philadelpia, United States.

Figure 20. DSC Q2000 testing machine.

For this work, the various thermal properties analysed were the following:

T_g	Glass transition temperature (°C)
T_{cc}	Cold crystallisation peak temperature (°C)
T_c	Crystallisation peak temperature (°C)
ΔH_c	Enthalphy of crystallisation (J/g)
T_m	Peak melting temperature (°C)
ΔH_f	Enthalpy of fusion (J/g)
X_c	Degree of crystallinity (%)

There are ways of predicting the results of a DSC test from knowing the structure and bonding of the investigated polymer. If there is cross-linking involved, one would expect a higher glass transition temperature as rotational movement is made harder [42]. The stiffness of functional groups as well as the backbone chains also decreases its flexibility, leading to an increase in glass transition temperature. Having double or triple bonds as well as dipole-dipole interactions increase the amount of energy needed to allow

the polymer chains to move freely. In the case of PET, it is generally not cross-linked but has a relatively stiff backbone chain with an aromatic group, it is expected to show a relatively high glass transition temperature.

The experiments related to this report used 5-6 mg of each material which was inserted in an enclosed aluminium capsule. To study the degradation produced by the compression moulding, both the pellets produced from extrusion and the plates produced from the compression moulding were investigated and compared. The protocol that was used for the DSC testing was a first heating, followed by a cooling and then finally a second heating. Each of these were performed with a temperature change of 10°C/min. The specifics of the protocol are detailed in Table 8.

Table 8. Protocol of DSC testing

Step	Description
1	2-minute stabilisation at starting temperature (20°C)
2	Linear temperature increase from 20°C to 290°C at 10°C/min
3	2-minute stabilisation at 290°C
4	Linear temperature decrease from 290°C to 20°C at 10°C/min
5	2-minute stabilisation at 20°C
6	Linear temperature increase from 20°C to 290°C at 10°C/min

Figure 21 shows the expected curve produced from the first heating cycle when performing a DSC with PET. It also shows how each thermal characteristic is determined from the heat flow vs. temperature curve.

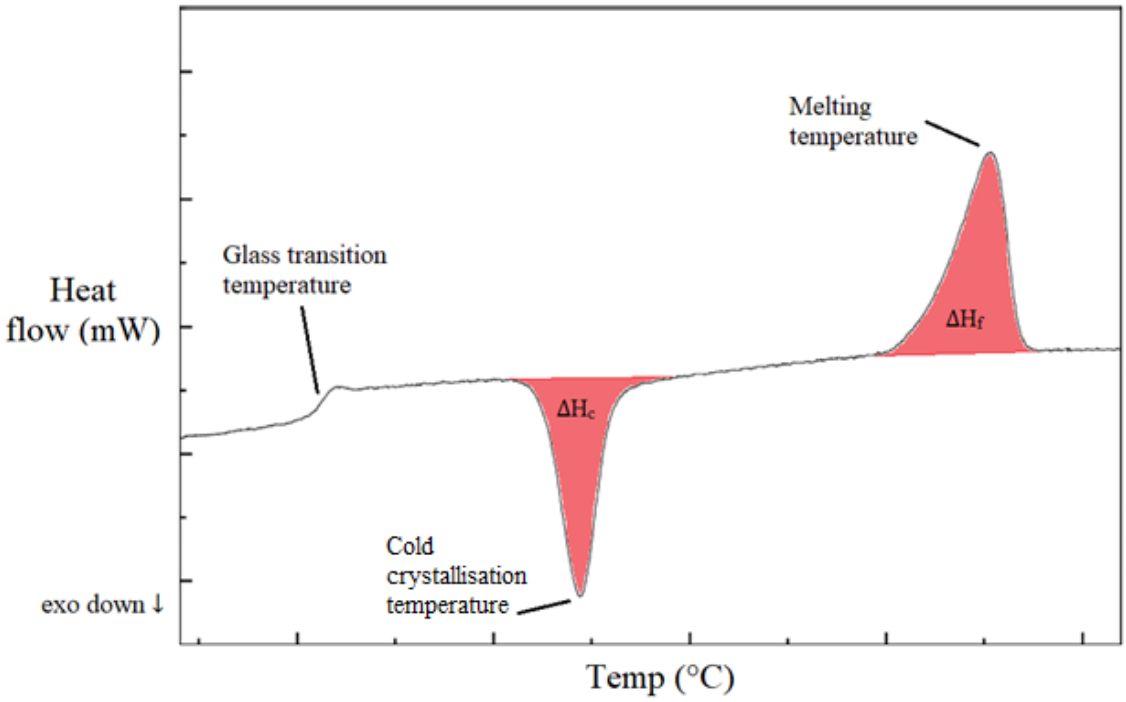

Figure 21. Traditional first heating DSC results from PET.

Note that X_c, the degree of crystallinity [%], can be determined thanks to the formula relating ΔH_f and ΔH_c with $\Delta H_f°$, the heat of fusion of a theoretically 100% crystalline sample taken at the equilibrium temperature, $T_m°$ [43]. Note that this work does not use pure PET, but rather PET with inclusions of solid TiO_2 particles. Accordingly, $f(TiO_2)$ is the fraction of inorganic particles found through calcination, in this work equal to 2.04%. The equation below takes this into account.

$$X_c\ [\%] = \frac{\Delta H_f - \Delta H_c}{\Delta H_f°(1 - f(TiO_2))} \times 100 \qquad \text{Eq. 13}$$

The numerical value of $\Delta H_f°$ [44] for PET is $\Delta H_f° = 140.1\ J/g$.

5.4. Tensile test

The samples for the uniaxial tensile testing were acquired from die-cutting the plates produced from the compression moulding according to chapter 4.3. The standard followed was ISO 527-2 [45] with samples of specimen 1BA. The dimensions for these are shown in Figure 22 and Table 9.

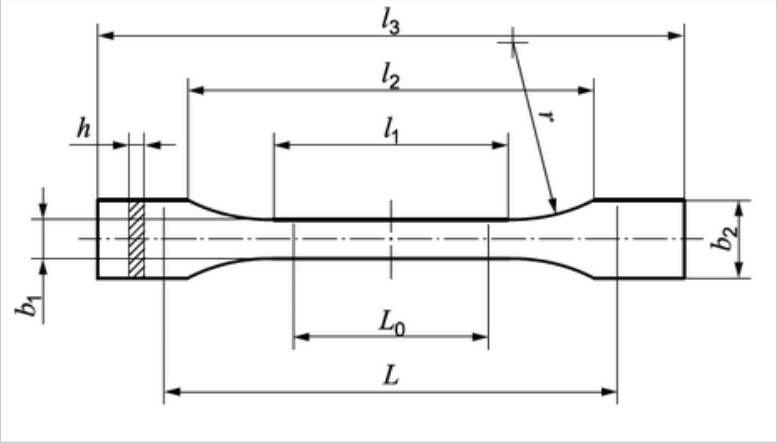

Figure 22. Tensile testing specimen 1BA

Table 9. Dimensions for specimen 1BA used for tensile testing.

	Tensile test specimen 1BA	**ISO 527-2 [mm]**
l_1	Length of reduced section	30.0 ± 0.5
l_2	Distance between shoulders	58.0 ± 2
l_3	Total length of the sample	≥ 75
r	Radius	≥ 30
b_1	Width of reduced section	5.0 ± 0.5
b_2	Width of grip end	10.0 ± 0.5
h	Thickness	≥ 2
L_0	Gauge length	25.0 ± 0.5
L	Initial distance between grips	l2 + 2.0

It should be noted that the thickness of the plates was less than what was specified in the norm, averaging at 0.44mm. This was done to cool the plate down as quick as possible while quenching in the goal of minimising crystallisation and distortion after compression moulding.

The tensile testing in this work was done on a machine of model SUN-2500, Galdabini, Cardano al Campo, Italy. It was equipped with a load cell of 1kN and the tests were performed with a constant crosshead speed of 10 mm/s. There was preloading done at 1.5N to be able to start the testing directly in the material's elastic region.

Figure 23. Galdabini Sun 2500 tensile testing machine. On the right is the camera for the video extensometer.

The primary data obtained from tensile testing is that of applied force (F [N]) and deformation (ΔL [mm]). Therefore, to obtain the engineering stress vs engineering strain ($\sigma_i \; vs. \; \varepsilon_i$) curves, the following equations are used to convert the data.

$$\sigma_i = F_i / A_0 \qquad \text{Eq. 14}$$

$$\varepsilon = \frac{\Delta L}{L_0} = \frac{L_x - L_0}{L_0} \qquad \text{Eq. 15}$$

A_0 [mm^2] is defined as the cross-sectional area of the reduced section of the sample, $A_0 = h \times b_1$, and L_0 [mm] is defined as the initial length before any force is applied.

Measurements of the deformation had two separate systems in place. The first was the software keeping track of the location of the crosshead and the second one the distance between two points on the sample

were tracked using video extensometer, model OS-65D, Mintron, Taipei, Taiwan. Given that the elastic deformation occurs in the zone between the two points, the gauge zone, the reading of the extensometer is considered to be more precise. For calculations of the Young's Modulus, therefore only the values from the extensometer are to be used. Due to practical limitations however, the video extensometer can only measure deformations below a certain value, meaning that for deformations outside the elastic region, the location of the crosshead is used for the rest of the acquired data. The value for L_0 varies for the two methods as the video extensometer only keeps track of the reduced region while the crosshead considers the entire sample. Therefore, L_0 is around 25mm for the video extensometer data and around 58mm for the crosshead data.

The characteristics that will be determined are the following:

E	Young's Modulus [GPa]
σ_y	Yield stress [MPa]
ϵ_y	Yield strain [%]
U_y	Yield energy [MJ/m3]
σ_{cd}	Cold-drawing stress [MPa]
ϵ_b	Strain at break [%]

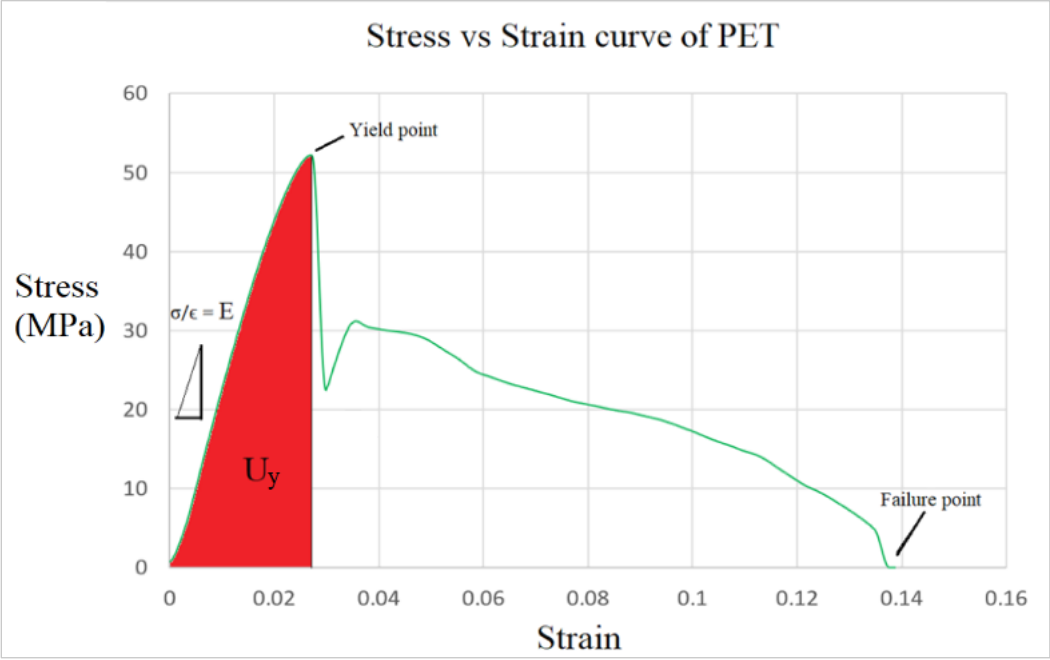

Figure 24. Example of an engineering stress vs engineering strain curve of ductile rPET-O.

Young's modulus and the yield energy are found through the following equations:

$$E = \frac{\sigma_2 - \sigma_1}{\varepsilon_2 - \varepsilon_1} \quad \text{Eq. 16}$$

$$U_y = \int_0^{\varepsilon_y} \sigma(\varepsilon) d\varepsilon \quad \text{Eq. 17}$$

In this work, since the Young's modulus is the slope of the engineering stress vs. engineering strain curve in the elastic region, it will be calculated using a linear regression between two points in the linear region. In Figure 24 it can be seen that for very low values of strain, there is not a linear relation as one would expect. To account for this and start directly in the linear region, a pre-load is applied. The calculation of Young's modulus must be done using points in the strictly linear region of the curve. The rest of the characteristics can all be determined graphically.

6. Results and discussion

6.1. Intrinsic Viscosity

The intrinsic viscosity of the various prepared materials with differing amounts of Joncryl as well as different processing conditions were measured. The results are shown in Table 10, combined with the estimations of the average molar mass using Mark-Houwink's equations.

Table 10. Results from intrinsic viscosity measurements.

	Pellets		**Plates**		
Material	η [dL/g]	$\overline{M_n}$ [gmol^{-1}]	η [dL/g]	$\overline{M_n}$ [gmol^{-1}]	η decrease (pellets to plates [%]
rPET-O	0.76	34 200	0.63	26 700	17
rPET-O+1J40	0.95	46 100	0.80	36 700	16
rPET-O+1J80	0.93	44 900	0.79	36 300	15
rPET-O+1.5J40	0.79	35 900	0.65	27 700	18

From the results, adding 1wt% of Joncryl chain extender increased the intrinsic viscosity by approximately 0.2 compared to rPET-O, an increase of around 25%. This means that the reactive extrusion was successful to some extent, as the hydrodynamic volume of the material had increased. The increase in rotation speed of the twin screw extruder decreased the intrinsic viscosity slightly, but with the uncertainty of the results

this is not enough to say with certainty that there was a definitive difference. However, since the results are so similar, one can determine that for the rPET-O+1J40 that the longer residence time and lower amount shear forces during reactive extrusion was balanced out by thermal degradation, causing the material to have approximately the same polymer chain lengths.

The addition of 1.5wt% Joncryl surprisingly decreased the intrinsic viscosity to levels similar to that of pure rPET-O. This could be explained by the increased number of branching sites associated with a higher concentration of Joncryl. Since the resulting polymer chains will be more branched than before, their hydrodynamic volume decreases and therefore also the measured intrinsic viscosity.

The results in this work are not similar to the ones presented in the previous master's thesis [1], as it was found that the intrinsic viscosity decreased with extra addition of Joncryl. This occurred for both transparent and opaque rPET. The suggested reason for this was that the Joncryl had promoted a three-arm or even six-arm star polymer structure (as can be seen in Figure 17) and therefore decreased its hydrodynamic volume. It was also found that the samples for opaque rPET with 1wt% and 1.5wt% Joncryl could not dissolve completely, leaving behind solid white particles. The suggested reason for this was that the reactive agent had introduced crosslinking to the PET, creating a dendrimer structure, as seen in Figure 17, and therefore was unable to be dissolved.

The difference in intrinsic viscosity between plates and pellets is notable. In all materials it was observed that the intrinsic viscosity decreased with around 0.13 dL/g and a percentage decrease of around 15%. This is to be expected as the plates were prepared in high temperature without an inert atmosphere, potentially causing thermooxidative degradation. In the technical data sheet of Joncryl® ADR 4400 [35] it is stated that the chain extender improves the hydrolytic stability of the polymer.

6.2. Rheometry

In Figure 25 and Figure 26, the graphs relating the storage modulus (G´) and the loss modulus (G´´) to the angular frequency (ω) are shown. Tests performed at 260°C.

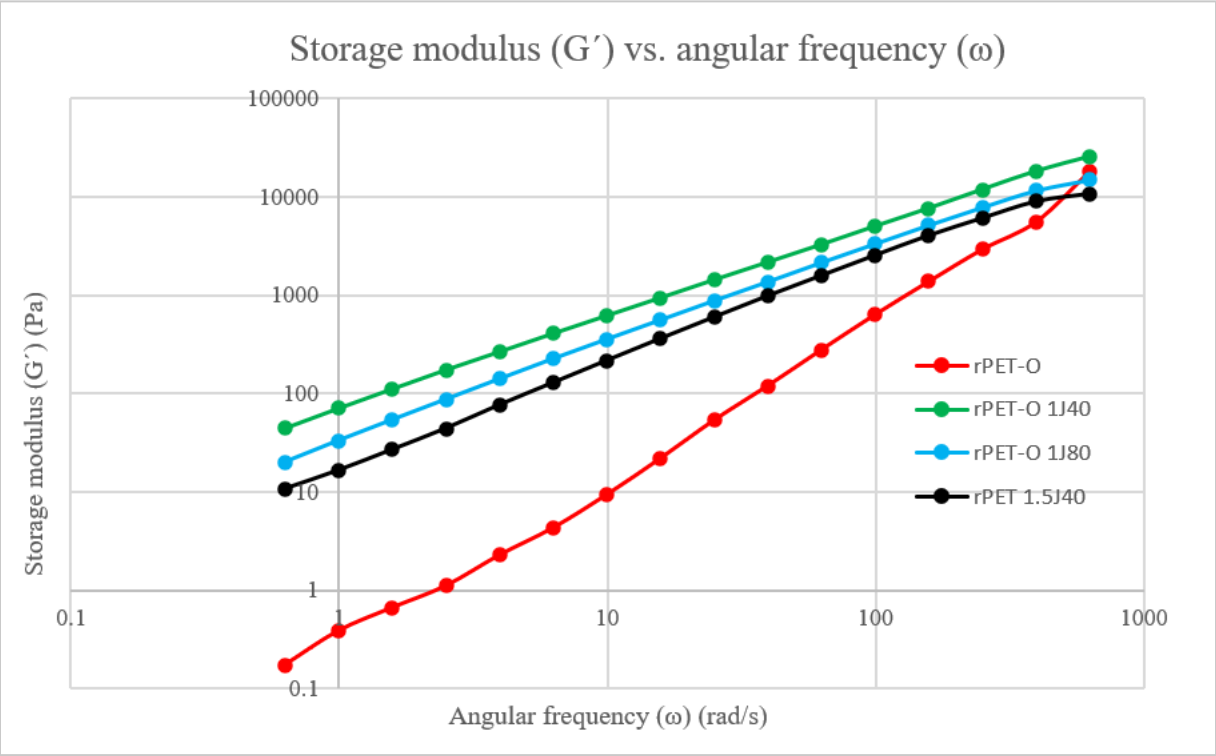

Figure 25. Results for storage modulus vs. angular frequency at 260°C.

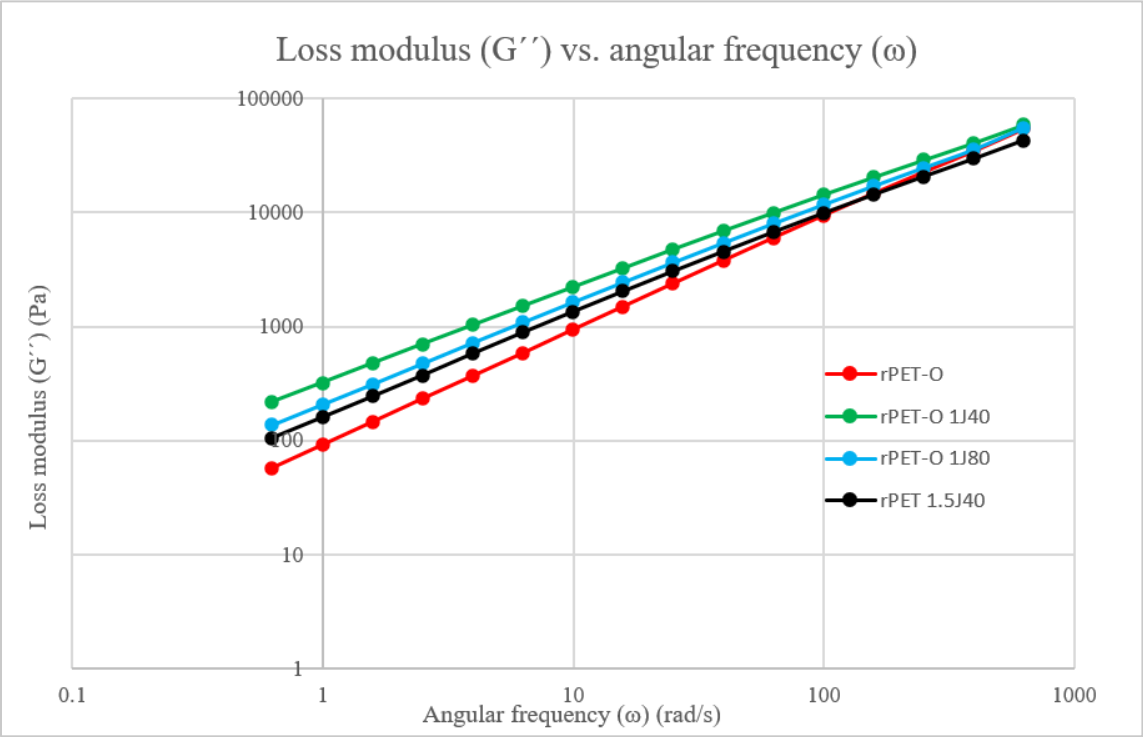

Figure 26. Results for loss modulus vs. angular frequency at 260°C.

In Figure 25 it can be seen that all materials having undergone reactive extrusion are relatively stable in its decrease of G´ with decreasing ω. However, the reference material, rPET-O, experienced some instability in this respect. As the material is subjected to high temperatures and shear forces, this could be due to degradation of the material during the test.

The slope of the log-log curve of G´ vs ω is close to 1 for all materials except rPET-O, which is likely because it is in the terminal zone. The other materials are all seemingly in the transition zone, means that they have more entanglement between their polymer chains, not allowing for rearrangement of chain conformation during each oscillation, indicating that branching during the reactive extrusion was successful.

Looking at the absolute values of G´, all reactively extruded materials possess an elastic proportion larger than that rPET-O. The highest effect from the reactive agent was had with rPET-O+1J40 and the lowest with rPET-O+1.5J40.

Figure 27 shows the relationship between η* and ω for the frequencies examined.

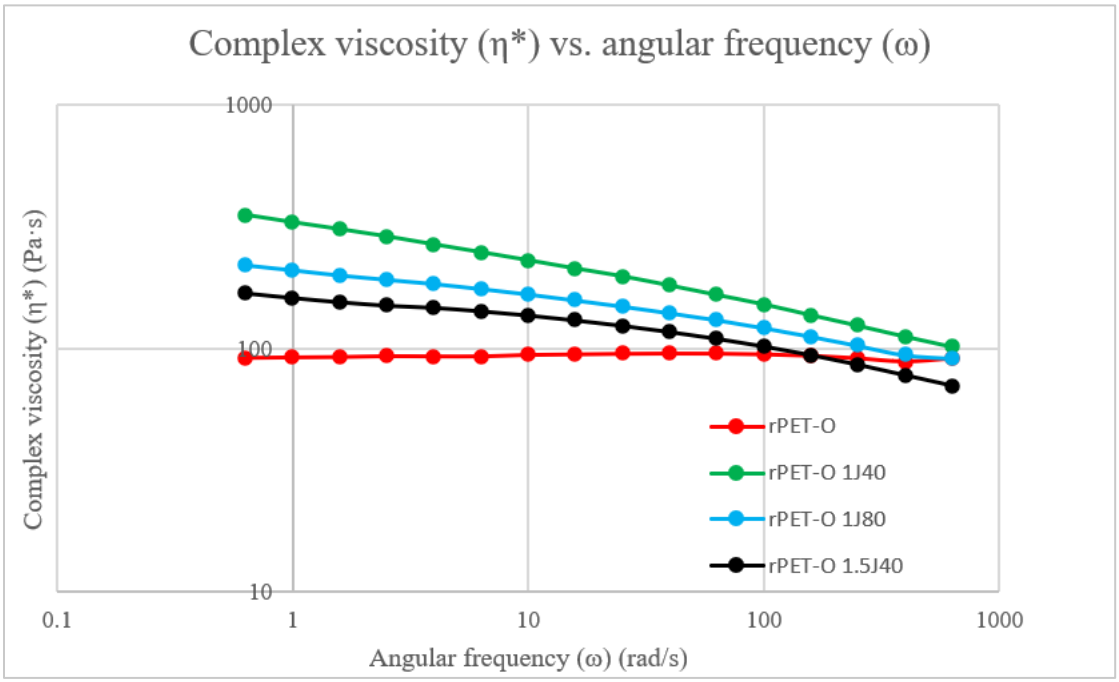

Figure 27. Results for complex viscosity (η*) vs. angular frequency (ω).

For the reference material rPET-O it can be seen that it displays close to Newtonian behaviour for the whole frequency range at 260°C. The other materials, however, display an increase in complex viscosity at lower angular frequencies.

Comparing the complex viscosities of the materials, it is clear that the sample with rPET-O+1J40 has the highest values at all points of testing.

The results are as predicted, as the longer residence time during reactive extrusion for rPET-O+1J40 creates more chain extension as well as branching and therefore more entanglements. For rPET-O+1.5J40 however this is not what is expected, as other researchers have found that the increased concentration of chain extender tends to lead to higher values of complex viscosity.

The results are mostly in accordance with what was found during the testing for intrinsic viscosity. It was expected that rPET-O+1J40 would show similar results as rPET-O+1J80, however for the rotational rheometry it showed more entanglement. This could be because even though there was a larger amount of branching, there was more thermal degradation occurring.

6.3. Differential Scanning Calorimetry

This sub-chapter will show the DSC graphs produced for each plate and combine analysis with the numerical values as displayed in Table 11.

Table 11. DSC Results for the different materials.

Plates	1st Heating				Cooling		2nd Heating			
	T_g (°C)	T_{cc} (°C)	T_m (°C)	X_c (%)	T_c(°C)	X_c (%)	T_g (°C)	T_{m1} (°C)	T_{m2} (°C)	X_c (%)
rPET-O	73	127	247	7	195	28	80	236	246	25
rPET-O+1J40	74	126	245	8	195	28	80	235	245	25
rPET-O+1J80	73	127	246	7	194	29	79	235	245	25
rPET-O+1.5J40	73	127	246	5	195	28	79	235	245	24

Figure 32 shows the heat flow vs. temperature graphs corresponding to each plate's first heating. As the glass transition temperatures were similar for each material, the peaks of cold crystallisation and melting are zoomed in.

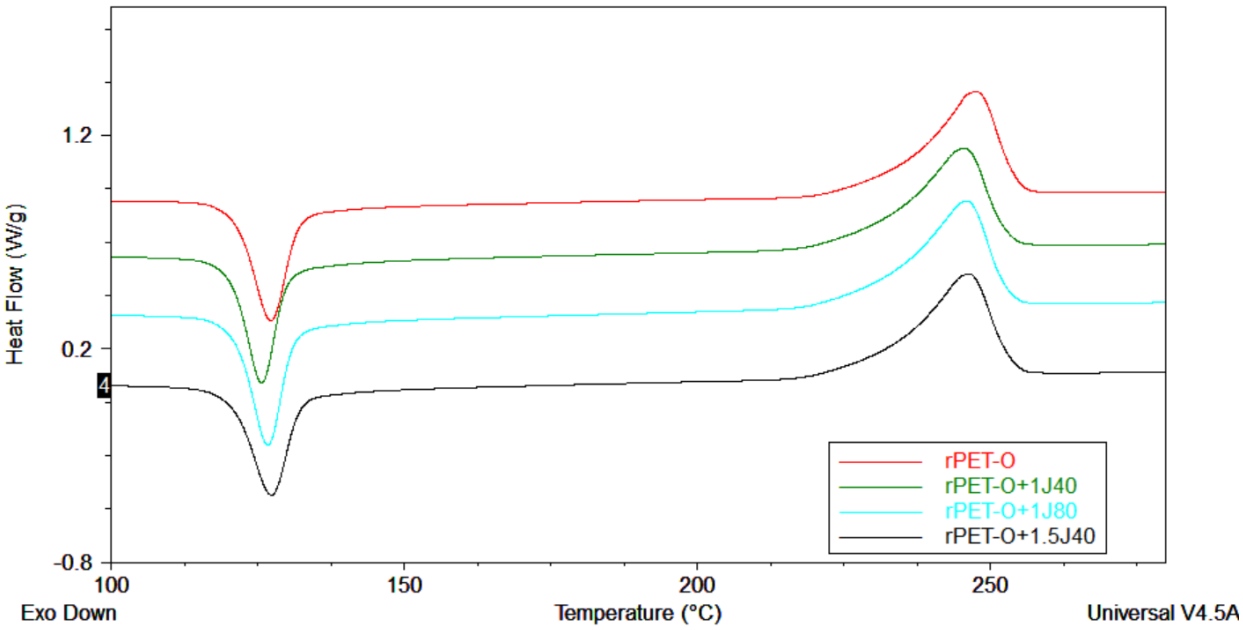

Figure 28. DSC of first heating of each plate.

During the first heating it can be seen that for the material with added reactive agent, both the cold crystallisation temperature as well as the melting temperature decrease. They decreased the most for rPET-O+1J40. This is coherent with the other results predicting that this material is the most entangled one, as chain linking and branching leads to less crystallising [46]. The material with the lowest degree of crystallinity is rPET-O+1.5J40. This could be explained by the fact that the Joncryl chain extender has a lower ability to form a crystal due to its different molecular structure from PET.

The plates, even though the process was designed to be able to cool down the plates as quick as possible, only 0.44mm in thickness and quenched in ice water, were still slightly semi-crystalline. This could be because the material shows a relatively high crystallisation ability, the points chosen for measurement of crystallinity are off, or because the moving of the plates from the hot press to the water being too slow. Unfortunately there was no visual indication of the degree of crystallinity as there would be with transparent PET.

Figure 29 shows the DSC for the cooling of the plates.

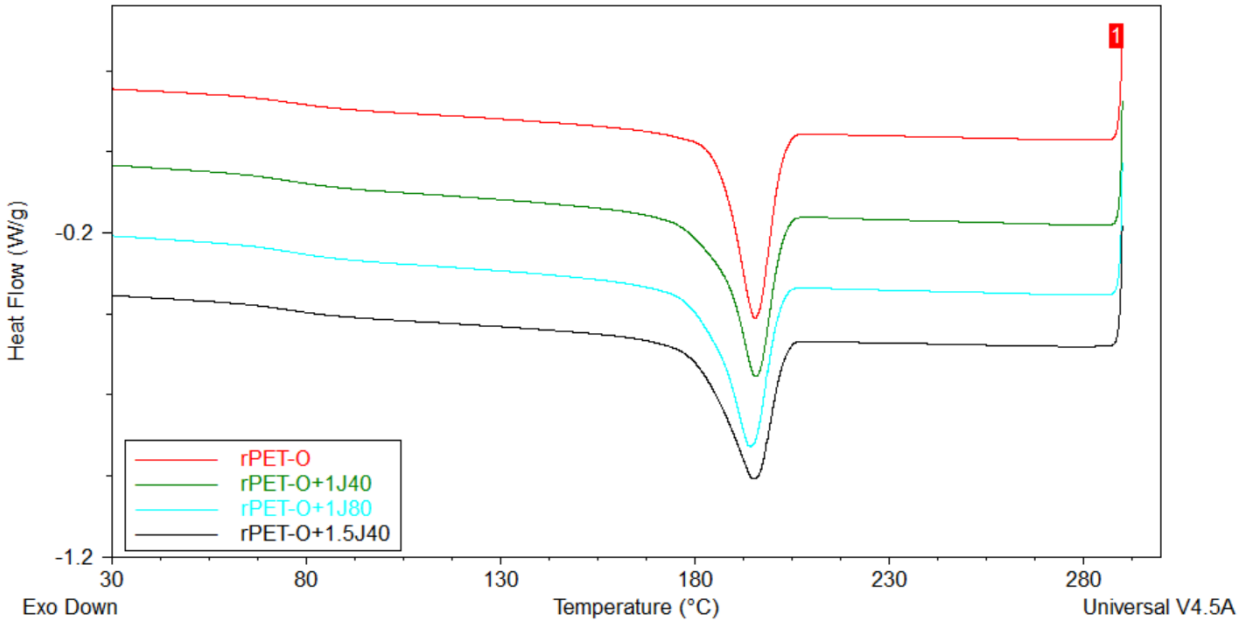

Figure 29. DSC results from cooling of each plate.

There was a small decrease in T_c for rPET-O+1J80 compared to the reference material but otherwise nothing noteworthy from these results. The cooling rate of 10K/min was sufficient to crystallise the sample to almost 30%.

Figure 30 shows the glass transition temperature and the multiple peaks for the melting temperature for each plate.

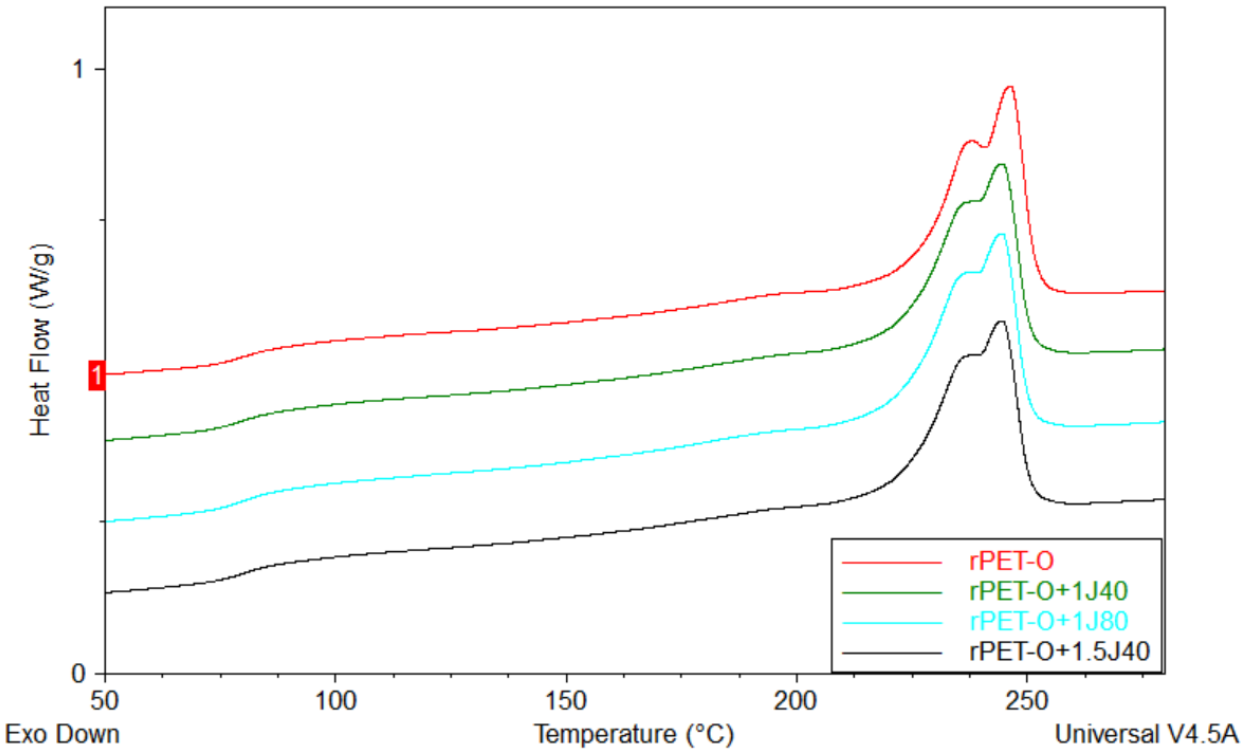

Figure 30. DSC results from the second heating of each plate.

The presence of multiple melting peaks is considered a normal phenomenon in semi-crystalline polymers. It has been suggested this is due to a recrystallisation after the initial melting, causing an exotherm, followed by the melting of these crystals, continuing the endotherm. [44] This is possibly due to different populations of lamellae, the first endotherm corresponding to the ones formed during crystallisation and the other to the ones formed through recrystallisation of fused lamellae during the heating process. It could also be because of the formation of larger crystalline sequences from amorphous sequences at the interface of the crystallites.

Regarding the impact of chain extender and the rotation speed during reactive extrusion, there were no major differences in the thermal properties across the different materials. The melting temperatures decreased slightly with the addition of Joncryl but the effect did not increase when the quantity increased to 1.5wt%. There was also minimal observed difference in the samples with different rotation speed during processing.

Comparing these results to the previous work [1], they are not in agreement. In that work there was a clear decrease in cold crystallisation temperature, crystallisation temperature and melting temperature when the amount of chain extender increased. This could be because of the reactive processing took place in an internal mixer, letting the rPET-O and Joncryl react longer and therefore form more clearly defined polymer structures.

6.4. Tensile testing

There were different mechanical behaviours from the materials as they displayed both brittle and ductile behaviour. The ductile samples themselves displayed two different behaviours, one where necking occurred without a stable propagation and another where necking followed by strain hardening occurred. For future purposes, these behaviours will be named brittle, ductile and CD-ductile, CD being the abbreviation for cold drawing. Typical engineering stress vs. strain curves of these three behaviours are shown in Figure 31. The brittle samples break directly after the yield point, the ductile ones which form necking after the yield point and the CD-ductile samples have stable propagation of the necking by strain hardening.

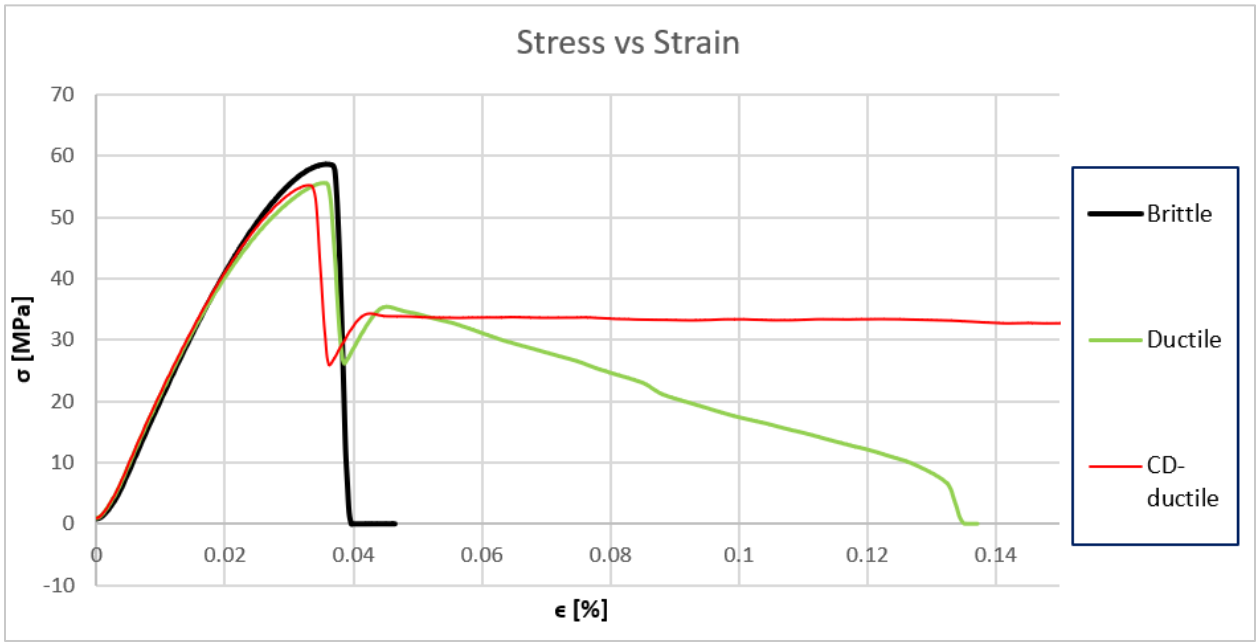

Figure 31. Typical engineering stress vs. strain curves for each mechanical behaviour displayed in this work.

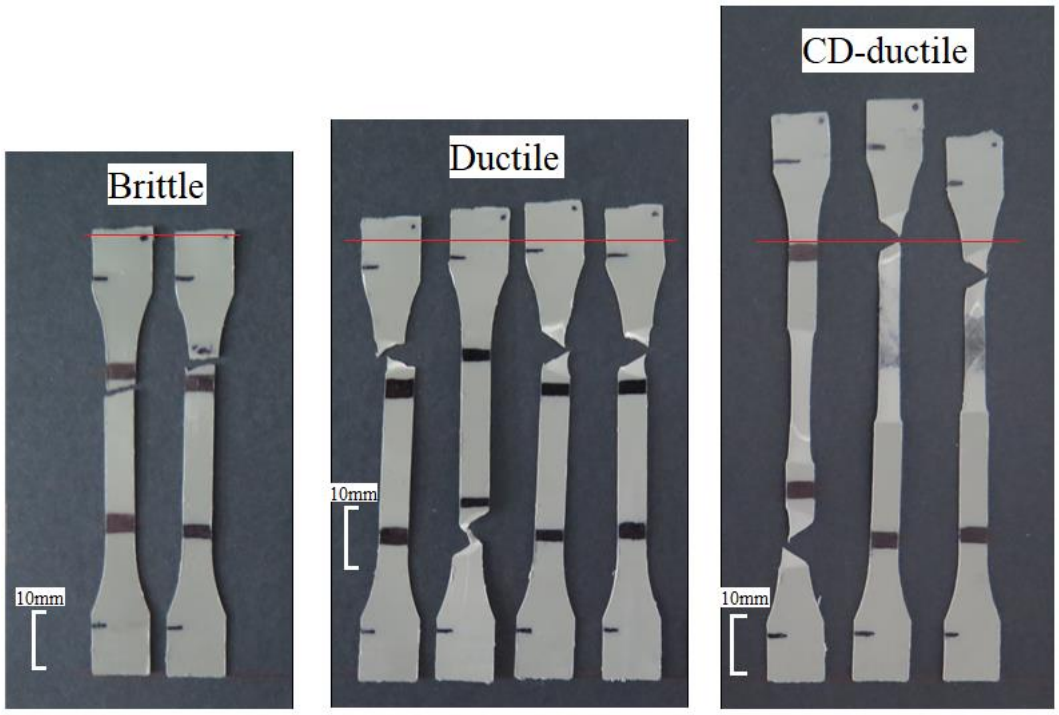

Figure 32. Tensile testing samples from rPET-O+1J40. The image shows the varying mechanical behaviour in the samples. The red line indicates the initial length of the sample.

As can be seen in Figure 32 and Table 12, from the 10 samples that were tested for each material, each material was able to show several different mechanical behaviours. The most occurring behaviour was the one chosen to be the representative one for each material.

Table 12. Frequency of brittle, ductile and CD-ductile behaviour in each material.

Material	Brittle (%)	Ductile (%)	CD-ductile (%)
rPET-O	60	40	0
rPET-O+1J40	22	44	33
rPET-O+1J80	40	40	20
rPET-O+1.5J40	100	0	0

rPET-O displayed mostly brittle behaviour and will therefore be considered as brittle. The samples for rPET-O with 1wt% added Joncryl displayed ductile and CD-ductile behaviour more than the other materials and will therefore be considered ductile. rPET-O+1.5J40 displayed only brittle behaviour. Figure 33 shows the representative engineering stress vs. strain curves for each material while Figure 34 is a photo showing the representative samples for each material.

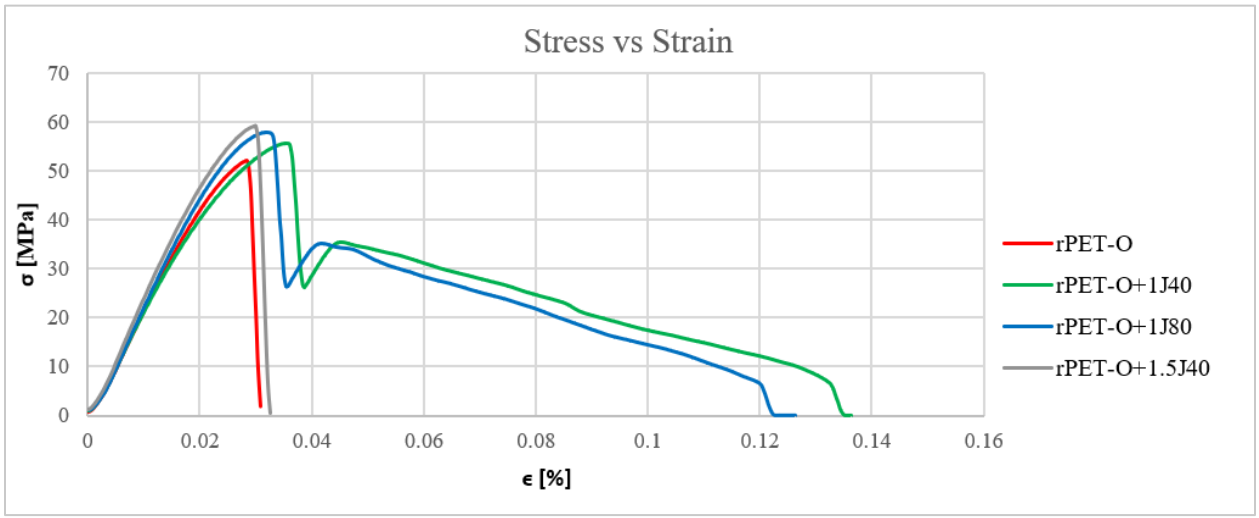

Figure 33. Representative engineering strain vs. stress curves for each material.

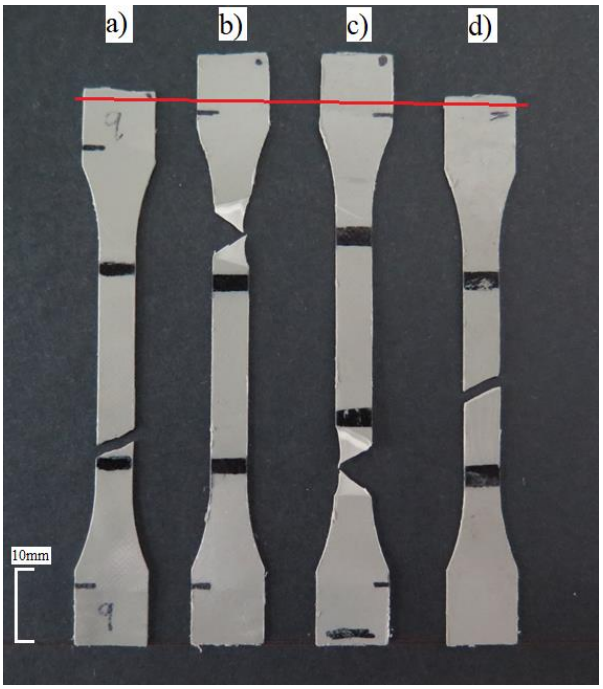

Figure 34. Representative samples of each material. The red line indicates the initial length of the sample. a) rPET-O. b) rPET-O+1J40. c) rPET-O+1J80. d) rPET-O+1.5J40

The numerical averages for each material were calculated and is presented in Table 13.

Table 13. Numerical results of tensile testing.

Material	E (GPa)	σ_y (MPa)	ϵ_y (%)	U_y (MJ/m3)	ϵ_b (%)
rPET-O	2.3 ± 0.1	53.1 ± 3.8	2.7 ± 0.1	0.8 ± 0.1	3.0 ± 0.1
rPET-O+1J40	2.4 ± 0.2	55.3 ± 2.9	3.2 ± 0.5	1.1 ± 0.2	11.4 ± 2.7
rPET-O+1J80	2.3 ± 0.1	57.0 ± 4.1	3.2 ± 0.3	1.0 ± 0.2	11.5 ± 1.6
rPET-O+1.5J40	2.4 ± 0.1	58.0 ± 1.0	3.0 ± 0.2	1.0 ± 0.1	3.2 ± 0.1

For any rPET-O modification by reactive extrusion, the yield strength and yield strain all increased. rPET-O+1J40 and rPET-O+1J80 both had the added benefit of being more ductile than the base material. They both had similar values of all mechanical properties investigated, as would be expected based on the previous results. Compared to the results of the previous work [1], the yield strength is higher but the yield strain is not. There it was found that both 1wt% and 1.5wt% added Joncryl promoted CD-ductile behaviour while in this work, only a few samples with 1wt% were seen strain hardening after necking.

The ability to strain harden was slightly higher in rPET-O+1J80, as can be seen in Figure 35 and Figure 36. The samples had an elongation at break of 120 ± 5 % compared to rPET-O+1J40 with only 44 ± 5 %. Following the results of the other tests, this can be explained by the molecules being less entangled and therefore orienting themselves more readily in the direction of the applied stress. The stress at cold drawing was similar for both materials at 32 ± 1 MPa.

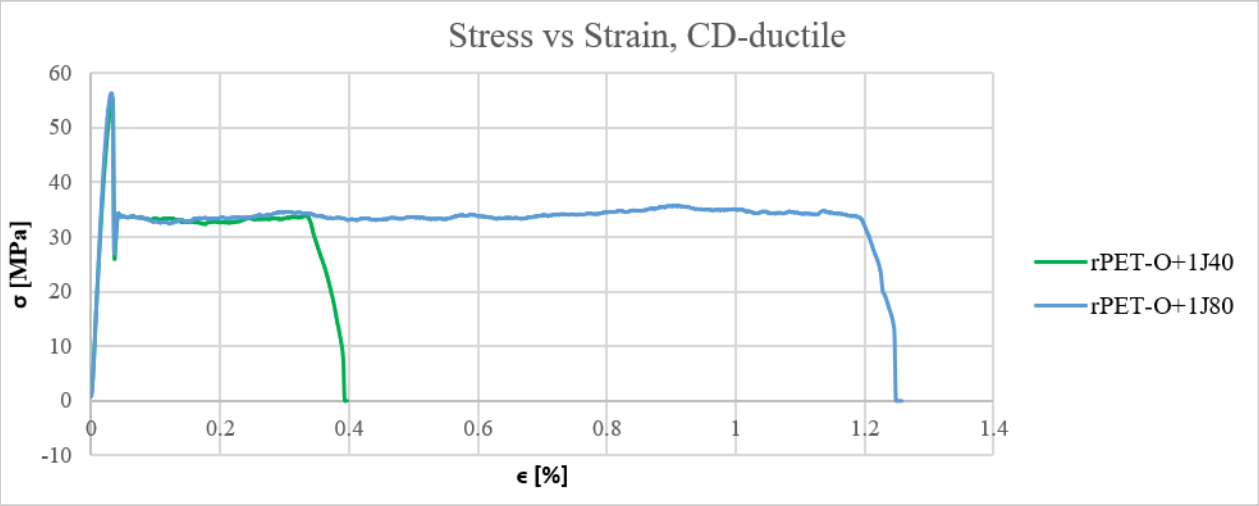

Figure 35. Engineering stress vs. strain curve for CD-ductile samples.

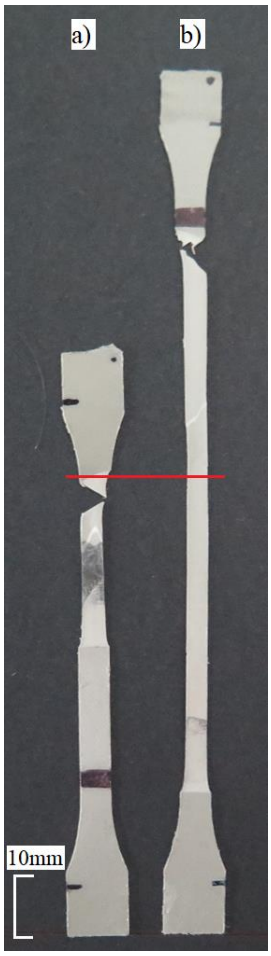

Figure 36. Samples with strain hardening after necking. The red line indicates the initial length of the sample. a) rPET-O+1J40. b) rPET-O+1J80.

To draw conclusions from the data that was produced it is relevant to combine the frequency of fracture behaviour with the actual results of the testing. As all samples for rPET-O+1.5J40 displayed fragile behaviour, it is fair to say that this material performed the worst out of the four examined. rPET-O showed a mostly fragile behaviour and in general had a lower strain and stress at the yield point. The material with the best results, albeit only slightly, was rPET-O+1J80. The properties were similar except for the ability to strain harden.

To find the reason for the dispersity of the different fracture behaviours, it would be recommended to analyse the samples using SEM analysis.

7. Conclusions

In this work, the optimal percentage of Joncryl to introduce for reactive extrusion with rPET-O was 1wt%. Increasing the rotation speed of the screws from 40rpm to 80rpm during reactive extrusion increased the mechanical properties slightly, even though the lower rotation speed produced more entanglement indicating that more had reacted. The intrinsic viscosity increased by around 0.20 dL/g (from 0.76 to 0.95 d) when adding 1wt% of Joncryl to rPET-O. The value barely increased at all for rPET-O+1.5J40. The rheological properties were the best for rPET-O+1J40, with a complex viscosity increasing by a factor of 4 compared to the reference material for low frequency oscillations. In terms of thermal properties there was not a large difference observed between the reference material rPET-O with adding Joncryl chain extender. A slight decrease in melting temperature was observed for all samples compounded with chain extender. The mechanical properties retrieved from the tensile testing revealed that the addition of 1wt% of Joncryl chain extender to rPET-O increased the ductility and tensile strength of the material slightly. This was the case for both materials with 1wt% addition of Joncryl, with a slight preference to rPET-O+1J80 due to its increased ability to strain harden. It was clear that adding 1.5wt% Joncryl to rPET-O made the material even more fragile and should not be an option to consider for future manufacturing.

The material rPET-O+1.5J40 had unexpected behaviour as it did not follow the trends from other works. It was a fragile material that did not seem to branch well at all. A suggestion is that there is some anti-synergistic effect in play above 1wt% of Joncryl, or simply that there was a mistake in introducing the Joncryl during the reactive extrusion. Ultimately why the material did not behave as expected can only be speculated.

It would be recommended to follow the same characterization protocol as described in this work but instead of using the compression moulding machine, use extruded sheets. This would be in order to avoid the extra step of possibly introducing thermal degradation each time the material is heated to or above its melting point. Since there was a dispersity in the results for the mechanical behaviour, morphological and fractographic analysis through SEM is recommended.

Analysis of environmental impact

The work presented is in the theme of circular economy, reusing a waste product to produce a material which has potential applications. That said, the machines, chemicals and materials that are used, all use

energy and need to be transported and therefore influence the carbon footprint. In this analysis, the potential factors of carbon dioxide emissions are considered. The software CCalc2 was used to get an approximation of the numerical values of each activity.

The production of raw material will be considered as non-polluting as it is a waste product. However, the transport must be taken into account. Around 50kg of raw PET flakes was used in this project, all transported from the south of France to Barcelona, equating to about 500km of transport. This is surpringly only emitting the equivalent of 1.5kg CO_2. This is because it was considered that the truck was transporting other goods at the same time.

The energy consumption will be investigated in the following paragraphs in a chronological order. Before the extrustion process, the material had to be dehumidified through heating. 0.6 kW is the energy consumption of the Piovan DPA6 which was used in the project. The dehumidification was done with 5kg raw material at a time and each lasted for 16 hours. This totals to 80 hours of running the dehumidifier. The energy consumption is therefore around 50kWh.

The extrusion process mainly requires energy for turning the screws and heating of each zone. It was estimated using data from Abeykoon et. Al [47]that the extrusion process requires 40kW to keep running. 5kg at a time was extruded, meaning in total 10 extrusions were performed, each for a duration of 3 hours. This would mean that the energy consumption for the extrusion process is around 1200kWh.

In the characterization part, the studied materials had to be dried in a vacuum oven at 80°C. Often this was done over-night as well, resulting in a drying time of 16 hours. From data sheets of related products, it is estimated to consume around 10kWh per day. Since many experiments were done on separate occasions, 10 days in total the machine had to be used. This results in an energy consumption of 100kWh.

The energy used for the machines related to compression moulding, DSC testing, tensile testing, RDA testing, the oven for recrystallisation and the freezer for the ice water quenching is considered to be negligeable compared to the previously mentioned processes. The total energy consumption for this project was around 1400kWh, with the largest contributor being the extrusion process. With data from the European Environment Agency [48], in Spain around 250g CO_2 is emitted per kWh. Thus, the CO_2 emissions from the energy used is around 360kg. Some neglected factors were the public transport travels from home to the university of the author, the air-conditioning, heating, and lights used in the building.

In terms of chemical disposal, this was a problem testing for intrinsic viscosity, the solvent 60/40 phenol/1,1,2,2-tetrachloroethylene was used to dissolve the PET. An estimated 300mg of this product was used, resulting in a negligeable CO_2-emission but carries with it a waste treatment problem. After its use, the solvent as well as the solution containing dissolved PET was disposed in a halogenated compounds waste container. The ethanol used to clean the glass capillary viscometer in between testing was also disposed in this same container. Gloves and paper in contact with the chemicals were disposed of in a separate waste container. These chemicals are not contaminating in terms CO_2-eq, but can pollute the earth in other ways such as freshwater eutrophication and terrestrial acidification if not handled correctly.

In conclusion, the carbon footprint for this is estimated to be around 360kg CO_2-eq.

Budget and cost analysis

The cost analysis will be done by looking at three factors:

1. Cost of materials.

The cost of materials will result in the lowest of the three, as the base material was a waste product its cost is effectively 0€. However, the cost of Joncryl chain extender and the solvent used in intrinsic viscosity testing. These materials are all relatively cheap compared to the costs associated with the other factors and will therefore be neglected.

2. Cost of using the machines for the preparation of the samples and for the characterization tests.

The cost of the machines is given by the hour and is an estimation based of the initial cost of investment, the cost of running it and its lifetime. The rates are given by the directrice of the Catalan Plastic Center, Dr. Maria Lluïs Maspoch Ruldua. The time used for each machine and the cost associated is presented in Table 14.

Table 14. Cost and use time of each machine during the project.

Machine	Cost	Use	Explanation	Total cost

Single-screw extruder (first two hours)	210€/hour	20 hours	10 extrusions in total	4 200€
Single-screw extruder (additional hours)	150€/hour	10 hours	Extrusions lasted 3 hours, one additional hour per extrusion	1 500€
Twin-screw extruder	210€/hour	10 hours	2 sessions of extrusion, each lasting 5 hours	2 100€
Dehumidifier	40€/hour	80 hours	16 hours per session of extrusion, 5 sessions in total	3 200€
Hot platen press (first plate)	200€/unit	3 units	2 days of training, 1 day of sample preparation	600€
Hot platen press (additional plates)	80€/unit	20 units	Training and sample preparation	1 600€
Intrinsic viscosity	240€/sample	10 samples	Training and testing	2 400€
Differential Scanning Calorimetry (first sample)	240€/sample	1 sample	-	240€
Differential Scanning Calorimetry (following samples)	150€/sample	7 samples	-	1 050€
Uniaxial tensile tests (first 10 samples)	200€/sample	10 samples	-	2 000€
Uniaxial tensile tests (following samples)	120€/sample	25 samples	-	3 000€
Rotational rheology (first sample)	330€/sample	1 sample	-	330€
Rotational rheology (following samples)	210€/sample	3 samples	-	630€

Summing up all total costs for the machines this puts the project at 22 850€.

3. Salary for workers.

The workload is shared between the author and the supervisors of the author. Assuming that the former is classified as a newly graduated engineer and the latter is classified as a senior engineer, the estimated time put into this thesis is estimated in Table 15.

Table 15. The number of hours put into each part of the project.

New engineer				**Senior engineer**	
Training	**Experimental work**	**Writing and documenting**	**Total**	**Training and proof-reading**	**Total**
200	400	200	800	100	100

The salary for a newly graduated engineer is assumed to be 30€ per hour, while a senior engineer is expected to earn 50€ per hour. This means that in total, the new engineer would cost 24 000€ and the senior engineer acting as a supervisor would cost 5 000€. In total, this factor costs around 29 000€ for this project.

Total cost:

Material cost	**Machine cost**	**Salaries**	**Total**
-	22 850€	29 000€	**51 850€**

Bibliography

[1] A. Lapuyade Cejudo, "Caracterización de PET Opaco Reciclado Mediante Extensión de Cadenas a Escala Laboratorio," M.S. thesis, Universitat Politècnica de Catalunya (EEBE), Barcelona, Nov. 2020.

[2] PlasticsEurope, "Plastics-the Facts 2019 An analysis of European plastics production, demand and waste data," Brussels, Belgium, 2019.

[3] Matthew Taylor, "Can Norway help us solve the plastic crisis, one bottle at a time?," Jul. 12, 2018. https://www.theguardian.com/environment/2018/jul/12/can-norway-help-us-solve-the-plastic-crisis-one-bottle-at-a-time (accessed Jan. 13, 2021).

[4] F. Welle, "Twenty years of PET bottle to bottle recycling - An overview," *Resources, Conservation and Recycling*, vol. 55, no. 11. pp. 865–875, Sep. 2011, doi: 10.1016/j.resconrec.2011.04.009.

[5] European PET Bottle Platform, "How to keep a sustainable PET recycling industry in Europe." https://www.epbp.org/ (accessed Jan. 13, 2021).

[6] "Factsheet - Opaque PET bottles and recycling," Kennisinstituut Duurzaam Verpakken, Oct. 2017.

[7] COTREP, "Note préliminaire - Impact du PET Opaque Blanc sur le Recyclage du PET," France, Nov. 2013.

[8] ZeroWaste France, "PET opaque-dossier complet." [Online]. Available: http://www.industrie.com/emballage/mediatheque/3/2/0/000019023.pdf.

[9] "Eco-profiles of the European Plastics Industry Polyethylene Terephthalate (PET) (Amorphous grade) I Boustead for PlasticsEurope Data last calculated," 2005. [Online]. Available: www.plasticseurope.org.

[10] F. Awaja and D. Pavel, "Recycling of PET," *European Polymer Journal*, vol. 41, no. 7. pp. 1453–1477, Jul. 2005, doi: 10.1016/j.eurpolymj.2005.02.005.

[11] PET Resin Association, "An Introduction to PET," Accessed: Jan. 20, 2021. [Online]. Available: http://www.petresin.org/.

[12] John. Scheirs and T. E. Long, *Modern polyesters : chemistry and technology of polyesters and copolyesters*. John Wiley & Sons, 2003.

[13] H. Köpnick, M. Schmidt, W. Brügging, J. Rüter, and W. Kaminsky, "Polyesters - Ullmann's Encyclopedia of industrial chemistry," in *Ullmann's Encyclopedia of Industrial Chemistry*, Weinheim, Germany: Wiley-VCH Verlag GmbH & Co. KGaA, 2000.

[14] Trudy. A. Dickneider, "Dupont's Technology For Polyester Regeneration." https://www.scranton.edu/faculty/cannm/green-chemistry/english/industrialchemistrymodule.shtml (accessed Jan. 13, 2021).

[15] T. Sang, C. J. Wallis, G. Hill, and G. J. P. Britovsek, "Polyethylene terephthalate degradation under natural and accelerated weathering conditions," *European Polymer Journal*, vol. 136. Elsevier Ltd, Aug. 05, 2020, doi: 10.1016/j.eurpolymj.2020.109873.

[16] Council of the EU, "Council adopts ban on single-use plastics," May 21, 2019. https://www.consilium.europa.eu/en/press/press-releases/2019/05/21/council-adopts-ban-on-single-use-plastics/?utm_source=dsms-auto&utm_medium=email&utm_campaign=Council+adopts+ban+on+single-use+plastics (accessed Jan. 13, 2021).

[17] M. Khoonkari, A. H. Haghighi, Y. Sefidbakht, K. Shekoohi, and A. Ghaderian, "Chemical Recycling of PET Wastes with Different Catalysts," *International Journal of Polymer Science*, vol. 2015. Hindawi Publishing Corporation, 2015, doi: 10.1155/2015/124524.

[18] S. Venkatachalam, S. G., J. V., P. R., K. Rao, and A. K., "Degradation and Recyclability of Poly (Ethylene Terephthalate)," in *Polyester*, InTech, 2012.

[19] M. Paci and F. P. la Mantis, "Competition between degradation and chain extension during processing of reclaimed poly(ethylene terephthalate)," 1998.

[20] M. Ahmadlouydarab, M. Chamkouri, and H. Chamkouri, "Compatibilization of immiscible polymer blends (R-PET/PP) by adding PP-g-MA as compatibilizer: analysis of phase morphology and mechanical properties," *Polymer Bulletin*, 2019, doi: 10.1007/s00289-019-03054-w.

[21] L. Sangroniz *et al.*, "Polyethylene terephthalate/low density polyethylene/titanium dioxide blend nanocomposites: Morphology, crystallinity, rheology, and transport properties," *Journal of Applied Polymer Science*, vol. 136, no. 4, Jan. 2019, doi: 10.1002/app.46986.

[22] N. C. Abdul Razak, I. M. Inuwa, A. Hassan, and S. A. Samsudin, "Effects of compatibilizers on mechanical properties of PET/PP blend," in *Composite Interfaces*, Oct. 2013, vol. 20, no. 7, pp. 507–515, doi: 10.1080/15685543.2013.811176.

[23] C. Yus *et al.*, "The effect of titanium dioxide surface modification on the dispersion, morphology, and mechanical properties of recycled PP/PET/TiO2 PBNANOs," *Polymers*, vol. 11, no. 10, 2019, doi: 10.3390/polym11101692.

[24] M. Pracella, F. Pazzagli, and A. Galeski, "Reactive compatibilization and properties of recycled poly(ethylene terephthalate)/polyethylene blends," 2002.

[25] I. M. Inuwa, A. Hassan, S. A. Samsudin, M. K. M. Haafiz, and M. Jawaid, "Interface modification of compatibilized polyethylene terephthalate/polypropylene blends: Effect of compatibilization on thermomechanical properties and thermal stability," *Journal of Vinyl and Additive Technology*, vol. 23, no. 1, pp. 45–54, Feb. 2017, doi: 10.1002/vnl.21484.

[26] N. Z. Tomić and A. D. Marinković, "Compatibilization of polymer blends by the addition of graft copolymers," in *Compatibilization of Polymer Blends: Micro and Nano Scale Phase Morphologies, Interphase Characterization, and Properties*, Elsevier, 2019, pp. 103–144.

[27] M. Akbari, A. Zadhoush, and M. Haghighat, "PET/PP blending by using PP-g-MA synthesized by solid phase," *Journal of Applied Polymer Science*, vol. 104, no. 6, pp. 3986–3993, Jun. 2007, doi: 10.1002/app.26253.

[28] A. Tavares, D. Silva, P. Lima, D. Andrade, S. Silva, and E. Canedo, "Chain extension of virgin and recycled polyethylene terephthalate," *Polymer Testing*, vol. 50, 2016, doi: 10.1016/j.polymertesting.2015.11.020.

[29] P. Raffa, M. B. Coltelli, S. Savi, S. Bianchi, and V. Castelvetro, "Chain extension and branching of poly(ethylene terephthalate) (PET) with di- and multifunctional epoxy or isocyanate additives: An experimental and modelling study," *Reactive and Functional Polymers*, vol. 72, no. 1, pp. 50–60, Jan. 2012, doi: 10.1016/j.reactfunctpolym.2011.10.007.

[30] D. Berg, K. Schaefer, and M. Moeller, "Impact of the chain extension of poly(ethylene terephthalate) with 1,3-phenylene-bis-oxazoline and N,N′-carbonylbiscaprolactam by reactive extrusion on its properties," *Polymer Engineering and Science*, vol. 59, no. 2, pp. 284–294, Feb. 2019, doi: 10.1002/pen.24903.

[31] I. Duarte *et al.*, "Chain extension of virgin and recycled poly(ethylene terephthalate): Effect of processing conditions and reprocessing," *Polymer Degradation and Stability*, vol. 124, 2016, doi: 10.1016/j.polymdegradstab.2015.11.021.

[32] K. Bocz, B. Molnár, G. Marosi, and F. Ronkay, "Preparation of Low-Density Microcellular Foams from Recycled PET Modified by Solid State Polymerization and Chain Extension," *Journal of Polymers and the Environment*, vol. 27, no. 2, pp. 343–351, Feb. 2019, doi: 10.1007/s10924-018-1351-z.

[33] F. N. Cavalcanti, E. T. Teófilo, M. S. Rabello, and S. M. L. Silva, "Chain extension and degradation during reactive processing of PET in the presence of triphenyl phosphite," *Polymer Engineering and Science*, vol. 47, no. 12, pp. 2155–2163, Dec. 2007, doi: 10.1002/pen.20912.

[34] Y. Zhang, W. Guo, H. Zhang, and C. Wu, "Influence of chain extension on the compatibilization and properties of recycled poly(ethylene terephthalate)/linear low density polyethylene blends," *Polymer Degradation and Stability*, vol. 94, no. 7, pp. 1135–1141, Jul. 2009, doi: 10.1016/j.polymdegradstab.2009.03.010.

[35] "Joncryl ® Functional Additives Joncryl ® ADR 4400 Polymeric Chain Extender for Food Contact Applications." Accessed: Jan. 20, 2021. [Online]. Available: http://www.nanozon.cn/UpLoadFile/file/20180910/6367219601961535158164833.pdf.

[36] S. L. Schmidt, K. Barker, and R. S. Adams, "Method and apparatus for determining moisture content," 1999.

[37] Y. Lu, L. An, and Z. G. Wang, "Intrinsic viscosity of polymers: General theory based on a partially permeable sphere model," *Macromolecules*, vol. 46, no. 14, pp. 5731–5740, Jul. 2013, doi: 10.1021/ma400872s.

[38] H. H. Chuah, D. Lin-Vien, and U. Soni, "Poly(trimethylene terephthalate) molecular weight and Mark±Houwink equation." [Online]. Available: www.elsevier.nl/locate/polymer.

[39] S. Farah, K. R. Kunduru, A. Basu, and A. J. Domb, "Molecular Weight Determination of Polyethylene Terephthalate," in *Poly(Ethylene Terephthalate) Based Blends, Composites and Nanocomposites*, Elsevier Inc., 2015, pp. 143–165.

[40] Malvern Instruments Limited, "A Basic Introduction to Rheology Shear Flow," 2016.

[41] S. Bair, T. Yamaguchi, L. Brouwer, H. Schwarze, P. Vergne, and G. Poll, "Oscillatory and steady shear viscosity: The Cox-Merz rule, superposition, and application to EHL friction," *Tribology International*, vol. 79, pp. 126–131, 2014, doi: 10.1016/j.triboint.2014.06.001.

[42] Pavan M. V. Raja and Andrew R. Barron, "Physical Methods in Chemistry and Nano Science - DSC Characterization of Polymers," Aug. 12, 2012. https://cnx.org/contents/uieDnVBC@25.2:3IZ8GyN5@1/DSC-Characterization-of-Polymers (accessed Jan. 13, 2021).

[43] Y. Kong and J. N. Hay, "The measurement of the crystallinity of polymers by DSC." [Online]. Available: www.elsevier.com/locate/polymer.

[44] H.-L. Chen, J. C. Hwang, and C.-C. Chen, "Multiple melting and crystal annealing of poly(ethylene terephthalate) in its blends with poly(ether imide)," 1996.

[45] ISO/TC 61/SC 2 Mechanical behavior, "ISO 527-2:2012 — Determination of tensile properties — Part 2: Test conditions for moulding and extrusion plastics," Feb. 2012. https://www.iso.org/standard/56046.html (accessed Jan. 14, 2021).

[46] S. Makkam and W. Harnnarongchai, "Rheological and mechanical properties of recycled PET modified BY reactive extrusion," in *Energy Procedia*, 2014, vol. 56, no. C, pp. 547–553, doi: 10.1016/j.egypro.2014.07.191.

[47] C. Abeykoon, A. L. Kelly, E. C. Brown, and P. D. Coates, "The effect of materials, process settings and screw geometry on energy consumption and melt temperature in single screw extrusion," *Applied Energy*, vol. 180, pp. 880–894, Oct. 2016, doi: 10.1016/j.apenergy.2016.07.014.

[48] European Environment Agency, "CO2 emission intensity," 2016. https://www.eea.europa.eu/data-and-maps/daviz/co2-emission-intensity-5 (accessed Jan. 14, 2021).